

Designing, Developing, and Validating Network Intelligence for Scaling in Service-Based Architectures based on Deep Reinforcement Learning

Paola Soto^{a,b}, Miguel Camelo^a, Danny De Vleeschauwer^c, Yorick De Bock^a, Nina Slamnik-Kriještorac^a, Chia-Yu Chang^c, Natalia Gaviria^b, Erik Mannens^a, Juan F. Botero^b, Steven Latré^a

^aUniversity of Antwerp - imec, IDLab, Sint-Pietersvliet 7, Antwerp, 2000, Belgium

^bUniversidad de Antioquia, Calle 67 No. 53-108, Medellín, Colombia

^cNokia Bell Labs, Copernicuslaan 50, Antwerp, 2018, Belgium

Abstract

Automating network processes without human intervention is crucial for the complex 6G environment. This requires zero-touch management and orchestration, the integration of Network Intelligence (NI) into the network architecture, and the efficient lifecycle management of intelligent functions. Reinforcement Learning (RL) plays a key role in this context, offering intelligent decision-making capabilities suited to networks' dynamic nature. Despite its potential, integrating RL poses challenges in model development and application. To tackle those issues, we delve into designing, developing, and validating RL algorithms for scaling network functions in service-based network architectures such as Open Radio Access Network (O-RAN). It builds upon and expands previous research on RL lifecycle management by proposing several RL algorithms and Reward Functions (RFns). Our proposed methodology is anchored on a dual approach: firstly, it evaluates the training performance of these algorithms under varying RFns, and secondly, it validates their performance after being trained to discern the practical applicability in real-world settings. We show that, despite significant progress, the development stage of RL techniques for networking applications, particularly in scaling scenarios, still leaves room for significant improvements. This study underscores the importance of ongoing research and development to enhance the practicality and resilience of RL techniques in real-world networking environments.

Keywords: 6G, Deep Reinforcement Learning, Model Evaluation, Validation, and Selection, Network Intelligence, Orchestration of Network Intelligence, Scaling Techniques.

1. Introduction

The upcoming 6G networks will face challenging and diverse objectives, such as offering Quality of Service (QoS) while guaranteeing Quality of Experience (QoE), infrastructure optimization, and scalable resource utilization. To face these challenges, these networks necessitate advanced automation beyond simplistic rules and heuristics [1]. Recognizing this complexity, Artificial Intelligence (AI) and Machine Learning (ML) are acting as main enablers for network automation and, ultimately, for providing the network with self-X (where "X" can stand for healing, configuration, management, optimization, and adaptation) capabilities [2, 3].

By embedding intelligence across all layers and throughout the entire lifecycle of communication services, the telco industry will transition towards an AI-native environment. The primary objective is to enable highly autonomous networks guided by high-level policies and rules. Emphasizing closed-loop operations and leveraging AI and ML techniques, the creation of Network Intelligence (NI) emerges as a pipeline of efficient algorithms for rapid response to network events [4], enabling autonomous network operations, and minimizing human intervention [5].

This transition will offer new opportunities for service provisioning but also introduce technical and business challenges. NI should be fully integrated into the network, where an orchestrator supports the

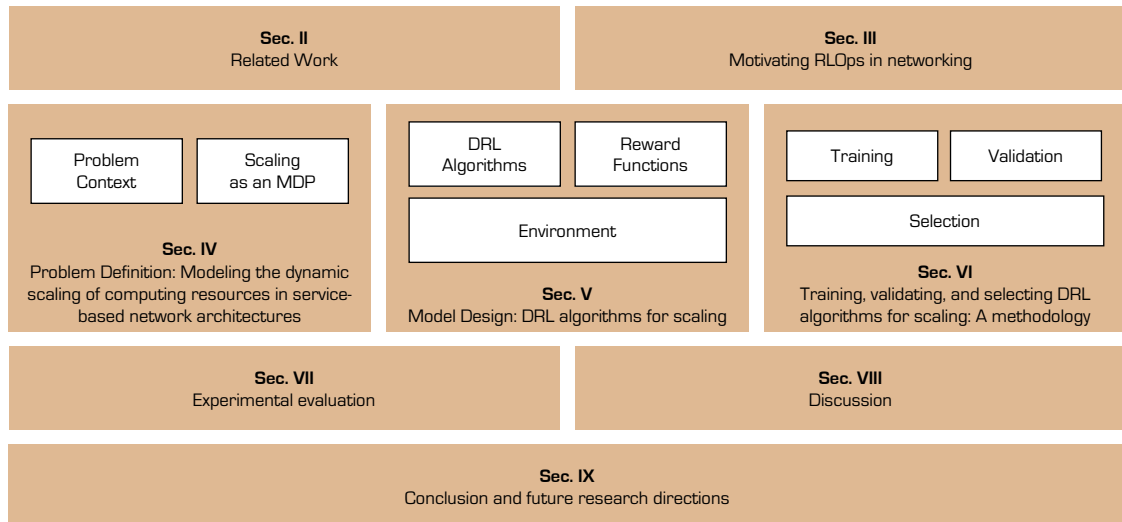


Figure 1: Overview of the organization of the paper.

orchestration and management of such AI/ML models [6]. In general, appropriate workflows for NI life-cycle management should be provided [7], which require the alignment with Machine Learning Operations (MLOps) practices [8]. The existing MLOps frameworks strive to automate and operationalize ML processes, ensuring the delivery of production-ready software. The workflow is intended to be model- and platform-agnostic. Nevertheless, to achieve a truly native NI integration into the network, automating the entire ML pipeline necessitates a harmonious integration between MLOps frameworks with the network Management and Orchestration (MANO) frameworks.

However, this integration is very challenging in practice. On the one hand, common ML applications use well-defined input data such as images, text, or audio. Conversely, ML algorithms tailored for NI add extra complexity regarding data velocity and variety. For instance, NI applications like traffic classification may involve diverse input data types, ranging from images [9] to time series [10]. On the other hand, most of the MLOps implementations predominantly focus on Supervised Learning (SL), often neglecting comprehensive support for Reinforcement Learning (RL) algorithms [11]. Incorporating RL introduces additional challenges to the ML workflow in the aspects of algorithmic design, model development, and model operation.

Following the MLOps workflow (cf. Figure 2), in this paper, we show how the challenges, carefully discussed by Li et al. [11], come to life when using RL for networking. Properly tackling these challenges, as we intend to do in this paper, will allow 6G systems to be closer to a completely autonomous network operation which will improve the scalability, reliability, and performance of network services leveraged by AI/ML algorithms. The contributions of this paper are manifold.

- We propose, as a use case, the scaling of computing resources in service-based network architectures such as Open Radio Access Network (O-RAN) or Network Function Virtualization (NFV). This use case requires intelligent scalers since current approaches for scaling are based on Central Processing Unit (CPU) usage. However, under this approach, the correlation between Service Level Agreement (SLA), QoS parameters, scaling decision triggers, and learning metrics is not known, or it is difficult to model. For instance, Altaf et al. and Gotin et al. [12, 13] show that CPU utilization might not be the best metric for non-CPU intensive applications. We model the scaling problem as a Markov Decision Process (MDP) and propose two RL algorithms that autonomously determine the number of replicas under a given constraint and constantly changing environment.
- We design three Reward Functions (RFns) that are suitable to the problem. Different RFns can guide agents to explore distinct strategies to achieve their objectives. This exploration helps uncover a broader spectrum of potential solutions and can lead to more robust and adaptive learning. In

particular, sparse RFns are challenging for agents to learn effectively since the agents only receive a reward after executing a sequence of actions. In contrast, the other two RFns provide more frequent and informative feedback, facilitating faster learning and convergence. In addition, we explore how the agent balances competing goals. This is particularly important in multi-objective RL, where optimizing one objective may come at the cost of deteriorating another.

- We enhance the MLOps methodology by incorporating practices for algorithm selection and comparison. In contrast to prior methodologies such as MLOps [14], Reinforcement Learning Operations (RLOps) [11], Q-Model [15], and O-RAN workflows [16], our approach considers multiple RL models introduced above, tailored to solve a specific problem. Furthermore, these diverse RL models are configured with different RFns, introducing an additional challenge as we aim to optimize the lifecycle management for not just one but multiple algorithms. Moreover, we validate this methodology via extensive experimentation and performance evaluation.
- We propose a benchmark on which scaling agents can be tested, and their algorithms can be compared. The benchmark is built on top of well-known frameworks in RL research, such as Stable Baselines [17] and OpenAI Gym [18]. We open-sourced this benchmark with the agents as a baseline for further evaluating, comparing, and advancing RL algorithms and models. Furthermore, it can complement well-established gym environments for networking, such as [19].

The remainder of this paper is organized as sketched in Figure 1, which is divided into eight sections. Section 2 reviews some state-of-the-art approaches for scaling and RL benchmarking. Section 3 motivates the use of MLOps and its extension to RLOps in the networking perspective. Section 4 briefly explains scaling and how it can be modeled as an MDP. As RL is an approach to solve MDPs, in Section 5, we introduce the two Deep Reinforcement Learning (DRL) algorithms and define the three distinct RFns, how they were designed and the rationale behind each RFn. Moreover, we explain how we build the environment that serves as a benchmark scenario for the methodology of Section 6. Section 7 details the experiments we conducted to test and validate the methodology for model training, validation, and selection; in Section 8, we discuss the results. Finally, Section 9 concludes the paper.

2. Related work

This section explores the foundational literature in two main areas: RL techniques for scaling in service-based network architectures and benchmarks in ML and RL within networking. This examination of related work establishes a contextual framework, paving the way for the contributions and differentiators of our research.

2.1. Reinforcement Learning for Scaling

Scaling strategies involve tackling a multi-objective problem trying to balance two conflicting goals. On the one hand, services demand QoS and QoE guarantees, which can be met by assigning more resources to the service. On the other hand, resource provisioning can cause Operational Expenditures (OPEX), represented in the expenses to keep the service running, e.g., energy bills, and Capital Expenditures (CAPEX), represented in the expenses to acquire, upgrade and maintain physical assets. Therefore, to fulfill the levels of QoS and QoE that services require with the least resources is of utmost importance. This is where scaling plays a key role.

Scaling techniques are usually classified into reactive and proactive. Reactive scaling involves adjusting resources in response to observed variations. Conversely, proactive scaling necessitates the capacity to predict forthcoming workloads and their impact in the QoS metric, allowing the scheduling of resources in advance. Recently, ML strategies have emerged for the adaptable scaling of resources in service-based networks, leveraging their capacity to learn from data and past experiences. Predominantly, these strategies have focused on proactive scaling, harnessing historical data through techniques like time-series forecasting [20] and workload prediction [21]. While proactive scaling has demonstrated advantages in minimizing the boot-up time for new instances and reducing SLA violations, reactive scaling remains prevalent in the cloud

industry due to its simplicity, satisfactory performance, and low computational overhead. Additionally, predicting workload is straightforward when patterns are regular (e.g., daytime or peak hours on weekdays), but the accuracy of predictions may decline when faced with unforeseen workload patterns.

Different techniques have been explored over a decade, carefully reviewed in Lorido-Botran et al. [22] and Chen et al. [23] for scaling in cloud environments. Duc et al. [24] give a broader view on resource provisioning in edge-cloud computing using ML. Since scaling can be modeled as a decision-making problem, one of the most used techniques in recent state-of-the-art is RL. Moreover, RL techniques can learn from previous experiences without making any further assumptions regarding network conditions (i.e., environment) and workloads, which makes them more attractive to network researchers. Therefore, the focus of our review is on these kinds of techniques. However, for an in-depth analysis of such approaches, we recommend the reader to Garí et al. [25] where they reviewed RL-based scaling techniques in the cloud.

RL as a scaling technique has been explored in several works [26, 27, 28, 29, 30, 31]. For instance, Rossi et al. [26] proposed a model-based and a model-free RL algorithm for horizontal and vertical auto-scaling in a docker swarm environment. Regarding the model-free approach, they use *Dyna-Q*, a Q-Learning variant where the state transitions are simulated, speeding up the learning process. In the model-based approach, the authors directly solve the Bellman equation by estimating the transition probabilities using CPU utilization. Although *Dyna-Q* experiences slow convergence, the model-based approach adeptly learns the optimal adaptation policy following user-defined deployment objectives.

He et al. [27] show the potential of using RL for scaling decisions by considering the interrelationship between multiple replicas that are chained to compose a network service. In this case, the authors used a Graph Neural Network (GNN) to create chain-aware representations, and then, using RL, the scaling decisions are made based on the representations. The prototype is implemented in OpenNetVM, a high-performance platform for Network Service (NS) chaining, where offline training and online inference are carried out. The evaluation results show that the combination GNN-RL outperforms the baseline algorithms regarding overall system cost and packet processing rate. The reasons behind the improvement are based on the prototype’s ability to i) learn from past experiences, ii) better demand prediction thanks to the composite features, and iii) the incorporation of the global chain information into scaling decisions.

The authors in [28] propose an RL algorithm with QoS guarantees to control a Kubernetes (K8s) cluster, reducing the microservices response time up to 20%. The RL algorithm identifies the right threshold values for pod scaling, which are then fed to the K8s Horizontal Pod Autoscaler (HPA). For training purposes, the authors simulated the HPA by taking the CPU and memory logs of two pods and adding a random factor on the resource usage and response time to increase the dataset size. The results indicated that the agents successfully reduced response time below the QoS target while adhering to a specified CPU utilization goal.

Soto et al. [29] proposed a control-theoretic solution and DRL-based scaling solution. The comparison between these two agents yielded that despite the DRL slightly creating more replicas than the control-based agent, it significantly reduces the number of SLA violations. An extension of this work is presented in [30], where better agents were introduced. Moreover, the scaling problem is framed into the Monitor-Analyze-Plan-Execute over a shared Knowledge (MAPE-K) paradigm, allowing the decomposition of several scaling methods in a generic form. The comparison with the control-theoretic solution showed that the learning behavior of the RL-based scaler heavily depends on the RFn definition, where light variations of the RFn result in different behaviors, while the control-theory based scaler is more deterministic in the scaling decisions.

In [31], authors study the impact of microservice interdependencies in scaling mechanisms. They developed *gym-hpa*, a framework that integrates the popular OpenAI [18] platform, and a K8s cluster, allowing them to train RL agents on real cloud environments. Experimental findings demonstrate that the RL agents trained using the *gym-hpa* framework, on average, decrease resource usage by at least 30% and diminish application latency by 25% when compared to default scaling mechanisms in K8s.

2.2. Benchmarks in Reinforcement Learning

In ML, a benchmark refers to a standardized set of tasks, datasets, or performance metrics used to assess and compare the performance of different algorithms or models. The goal of a benchmark is to

provide a common ground for evaluating the effectiveness of various approaches in solving specific problems. Benchmarks are widely used in ML to measure algorithmic advancements, facilitate fair comparisons, and track the state-of-the-art in different subfields.

The main elements in a ML benchmark include well-defined tasks, carefully curated datasets, metrics to measure performance, evaluation protocols, and often baseline models for reference. Benchmarks define specific tasks or problems that algorithms are expected to solve. These tasks range from classification and regression to more complex challenges like image recognition and natural language processing. However, such tasks are related to SL approaches. Regarding RL, typical tasks are related to continuous or discrete control problems.

Concerning the datasets, benchmarks often include standardized datasets for training, validation, and testing. These datasets are carefully curated to represent the diversity and complexity of real-world scenarios, ensuring that algorithms are evaluated under realistic conditions. While SL approaches benefit from a wide range of datasets depending on the task [32, 33, 34], RL are evaluated using standard environments, where OpenAI Gym [18] is the most recognized. Three main types of environments are identified. Environments with discrete action spaces are evaluated using Atari video games, including Pong, Breakout, Space Invaders, Seaquest, and more. Moreover, for continuous action spaces, OpenAI Gym integrated the MuJoCo physics engine, where the action input applies torque on the joints of a humanoid robot learning to walk. Less complex environments include the classic control ones, which are stochastic in their initial state and are considered the easiest to solve by a RL algorithm.

Additional elements in a ML benchmark include the metrics used to quantify their performance. Common metrics include accuracy, precision, recall, F1 score, mean squared error, or area under the Receiver Operating Characteristic (ROC) curve, depending on the nature of the problem. Moreover, benchmarks also define the protocols for training and evaluating models. This includes guidelines on splitting the dataset into training and testing sets, whether cross-validation is used, and any specific considerations for model evaluation. Finally, benchmarks often include baseline models or algorithms that provide a reference point for comparison. These baselines help establish a performance threshold against which new algorithms can be measured.

Nevertheless, reproducibility of RL is hard to achieve, as shown in [35], where the authors performed a thorough study by implementing and comparing state-of-the-art DRL algorithms in the benchmarks provided by OpenAI Gym such as Half-Cheetah, Hopper, and Swimmer. They find out that different implementations of the same algorithm with the same hyperparameters can lead to distinct behaviors. Moreover, due to the lack of meaningful metrics and more stringent standardization in experimental reporting, discerning the significance of improvements over the previous state-of-the-art becomes challenging. Due to variance across trials, multiple runs with different random seeds are necessary for reliable comparisons. Proper significance testing, including bootstrapping and power analysis, is vital to validate performance gains. The key to reproducibility is thorough reporting of hyperparameters, implementation details, and experimental setup, as lacking this information hampers progress in RL research.

More focused on methods for continuous control, the authors in [36] examine the general variance of the algorithm’s performance depending on the initialization of their hyperparameters in policy gradients for continuous control and provide guidelines on reporting novel results against the baseline methods. By running extensive experiments, the authors found that state-of-the-art RL algorithms frequently exhibit significant variations due to differences in hyperparameter configurations. Moreover, outcomes in diverse continuous control domains do not consistently align, as demonstrated in the experimental results involving the Hopper and Half-Cheetah environments. Half-Cheetah’s performance is more susceptible to fluctuations from hyperparameter tuning, whereas Hopper does not exhibit the same sensitivity. According to their analysis, the under-reporting of hyperparameters may lead to unfair baseline comparison in continuous control environments.

In networking, standard implementation of RL algorithms is still in its infancy. An initial step involves establishing an abstraction layer that enables the representation of a network environment as a Gym environment. This layer exposes simulation entities’ states and control parameters for the agent’s learning objectives. An example of such an abstraction layer is shown in [19], where ns-3 [37], a known network simulator whose results are widely accepted by the networking research community, is used as a network en-

vironment. The main components of *ns3-gym* are two communicating processes that exchange information between frameworks using Google Protocol Buffers (Protobuf) [38] and ZeroMQ (0MQ) sockets. As a case study, the authors presented two examples of a cognitive radio transmitter that adapts its channel access patterns accordingly with a periodic interferer.

An extension of the previous work is made in [39], where they proposed a shared memory implementation to replace the Protobuf - 0MQ combination as a more efficient, high-speed way of communication. Moreover, thanks to their implementation, the ns-3 simulator can communicate with popular ML frameworks such as PyTorch and TensorFlow, including Deep Learning (DL) algorithms as well. Like the previous work, the authors showed the viability of *ns3-ai* by predicting the channel quality information in cellular systems to improve the channel estimation and the communications between users and base stations in 5G new radio.

More recently, Bonati et al. [40], presented *OpenRAN Gym*, an O-RAN compliant toolbox that combines several software frameworks for Radio Access Network (RAN) data collection and control. AI algorithms are deployed as xApps in the near real-time RAN intelligent controller, trained in Colosseum, the world’s largest wireless network emulator [41], and later can be seamlessly transferred to heterogeneous platforms. Utilizing the presented toolbox, the authors illustrated the application of two xApps for managing a large-scale O-RAN deployed on Colosseum. Furthermore, they highlighted the seamless transition of *OpenRAN Gym* solutions and experiments from the Colosseum to real-world platforms, including the Arena testbed, the POWDER, and COSMOS platforms within the PAWR program.

2.3. Differences with previous works

In previous subsections, we i) reviewed state-of-the-art techniques for scaling with special emphasis in RL approaches and ii) described common benchmarks in RL and reviewed the current body of literature regarding the integration of networking and RL.

On the one hand, the works showing RL techniques for scaling are opaque in reporting the work done at fine-tuning their RL agents. They lack a detailed overview of the parameters used in their agents, only show the results of their best-performing agent, or do not specify how many runs of the same algorithm they performed, a practice highly discouraged by RL practitioners since it hampers the reproducibility of such techniques and further development. An exception to this common practice in networking is our previous work [30], where we showed the impact of the RFn definition on the performance of the RL agent and the variability of its performance even using the same RFn.

On the other hand, there are growing efforts in designing frameworks that allow a common and standard way of training and evaluating RL algorithms for networking. Nevertheless, such efforts focus more on RAN implementations than on cloud-like environments. The ns-3 simulator puts more effort into simulating actual devices but lacks support for service-based network architectures. Several extensions are available but tailored to specific cases, such as Field Programmable Gate Arrays (FPGA) implementations for 5G networks [42] and O-RAN solutions [43], where the service management and orchestration module, in charge of the xApps lifecycle operations (scaling being one of them), is out of the scope of their model. Moreover, the work proposed by *OpenRAN Gym* is interesting since it created a platform to train and evaluate ML and RL models using large-scale emulators. However, since their interfaces do not follow the OpenAI Gym abstractions, it limits the benchmarking of RL algorithms and compatibility with future RL frameworks in other network domains.

With this work, we pretend to tackle the deficiencies mentioned above. Concerning the reproducibility issue, we thoroughly describe our training and testing procedures. Moreover, we follow the standard implementations of stable baselines, which already deliver the tuned hyper-parameters as intended in their original versions. Furthermore, we open-source our environment and abstraction layer for scaling in service-based network architectures, similar to the work done in [31]. Though, being a simulator, *DynamicSim* avoids the impracticality of owning or renting a K8s cluster, accelerating the learning curve of new RL in networking practitioners. We hope this work will foster research in the applicability of RL in networking and further adoption in real-life environments.

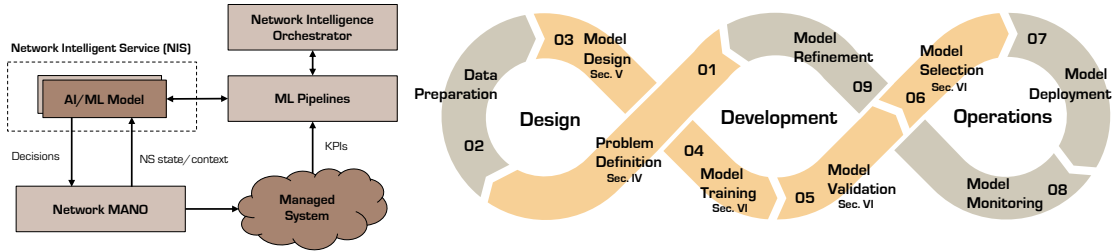


Figure 2: NI integration into future network architectures. On the left are the high-level interactions among the building blocks of an AI-native architecture for B5G networks [6]. On the right is a typical ML lifecycle, including three main phases: Design, Development, and Operations.

3. Motivating RLOps in networking

The integration of NI into future network architectures is essential and should be supported by an NI orchestrator for managing intelligent models [6]. Effective workflows for NI lifecycle management, aligned with MLOps practices are crucial [8]. Rooted in the “DevOps” concept, the MLOps frameworks embrace a methodology that advocates software automation through continuous integration, delivery, and deployment (CI/CD), facilitating swift, frequent, and reliable releases [14]. Both DevOps and MLOps align with the infinity model, emphasizing continuous product improvement, making them well-suited for software development, where the emphasis lies in incorporating new updates and features rather than complete product redesign. Figure 2 illustrates, on the right, a typical ML workflow.

For developing and operating Network Intelligent Service (NIS), the shown ML workflow should be applied alongside the NIS lifecycle. A key component in an AI-native architecture with autonomous operations is the NI orchestrator. This orchestrator is responsible for interpreting the user intentions (e.g., based on intent-based networking [44]), composing a NIS, deploying an appropriate AI/ML model, which guides the NIS behavior, and monitoring that the NIS behavior is as expected. To be able to do that, the NI orchestrator implements (on its own or via a third-party service) an ML workflow.

This workflow starts with the definition of the requirements, typically derived from the problem at hand. For instance, scaling can be solved through SL techniques, which implies the collection, curation, and maintenance of a historical database with historical scaling decisions and values of the Key Performance Indicators (KPIs) collected from the managed entity. However, scaling can also be solved through RL techniques (as it will be shown later in this paper), which implies the preparation of a sandbox [45] in which the RL agent can freely interact with a digital replica [46] of the managed system to train a scaling policy.

The next phase involves selecting an appropriate learning type and ML model. Continuing with the scaling example, multiple SL models could be employed as scaling agents depending on how the problem is posed. Scaling decisions can be seen as data sequences for which time series models can be used. Regarding the RL techniques, we provide a comprehensive discussion in Section 5, where one of the major difficulties resides in the RFn definition.

In the development phase, model training and fine-tuning occur, including tuning the model’s architecture and hyperparameters (e.g., learning rate, activation functions, and regularization methods). Following model construction, validation is performed by introducing unseen data to enhance generalization. Upon achieving a predefined performance, the NI orchestrator deploys the model as a Network Intelligent Function (NIF) inside the NIS. After deployment, the NI orchestrator continuously monitors the performance of the NIS. Typical quality metrics of ML models are accuracy, loss value, and average return after an epoch, among others. Nevertheless, the NI orchestrator could potentially be supported by metrics gathered from the managed system to assess the quality of the ML model. Continuous monitoring is vital due to potential data and model drift, ensuring service quality. If the model fails to meet quality standards, refinement is undertaken, restarting the cycle.

The existing MLOps frameworks strive to automate and operationalize ML processes, ensuring the delivery of production-ready software. The workflow is intended to be model- and platform-agnostic. However,

most of the MLOps implementations predominantly focus on SL, often neglecting comprehensive support for RL algorithms [11]. Incorporating RL introduces additional challenges to the ML workflow, encompassing four aspects.

Firstly, the problem to be addressed must be formulated as a MDP, where the learning goal of a RL agent is to find an optimal policy through the use of a RFn. By interacting with an environment, the RL agent gathers states and rewards, facilitating the iterative approximation or computation of the expected long-term reward, enabling the selection of optimal actions at each step. Unlike the intrinsic “labels” in SL, rewards reflect the anticipated behavior of agents. Consequently, the design of the RFn must be done carefully and sometimes requires specialized considerations.

Interactions and learning for RL algorithms still comes along with significant challenges due to network vulnerabilities. To ensure the safety of RL algorithm training, an offline approach is recommended [16]. In this offline setting, the RL agent accumulates experiences by exploring actions randomly, allowing it to learn without impacting network operations. To facilitate this learning process, Network Digital Twins (NDTs) are proposed to provide a controlled, reliable, and easily accessible simulation environment [46], enabling RL algorithms to safely explore new actions. Consequently, a parallel branch is required to support this learning type. In the primary branch, decisions from an already trained agent are implemented in the production network, while algorithms still undergoing training can introduce their outcomes in the NDT [6].

A third aspect challenging the full support of RL in MLOps frameworks is the reproducibility issue. It has been found that minor implementation details can considerably impact performance, sometimes surpassing the disparity between various algorithms [47, 36, 35]. Best practices in the RL community include the use of standard agent-environment interfaces [18], RL implementations [17] and full transparency in reporting the settings used when training RL algorithms. Unfortunately, such practices are not fully adopted in the growing body of literature of RL applications in networking [48].

Finally, a key feature of the NI orchestrator involves autonomously selecting and validating models. In a dynamic environment where various Network Operators (NOs) may develop their own AI/ML/RL models, multiple models could potentially be deployed for a single function. Hence, the orchestrator is crucial in determining which available model should be deployed, preventing conflicts, and optimizing resource utilization. Unfortunately, existing implementations of MLOps frameworks lack this feature, as their workflows are designed for a single model or perform manual model selection based solely on the learning metrics (e.g., loss, accuracy, or reward). However, as we will show in the following sections, RL algorithms should also be validated in terms of the performance of the task they are designed to solve.

In the following sections, we focus on the design and development phases of the workflow shown in Figure 2, paying special attention to the challenges we just mentioned when applied to the networking field. In particular, Section 4 poses the scaling problem as a MDP, setting the requirements for the environment and algorithm design, which are shown in Section 5. Section 6 focuses on the development part as it explains the difficulties when training and validating RL algorithms. Additionally, it proposes a methodology for performing model selection, an important step before its deployment in production networks.

4. Problem definition

This section focuses on the design phase of the MLOps workflow. Specifically, this section deals with the definition of the problem, where the dynamic scaling of computing resources in service-based network architectures is modeled. For doing this, we provide the context and necessary background information to understand the scaling problem and its implications in RL.

4.1. Problem Context and Description

The current and future networks are transitioning to a service-based architecture, where traditional Network Functions (NFs) are being replaced by small software pieces that can be enclosed into granular containers, able to run in Commercial Off-The-Shelf (COTS) hardware. Such functions can be composed so that a NS is constituted. Such granular decoupling has numerous benefits. The underlying infrastructure can be shared by multiple containers since, in the first place, containers are not designed to be run on specialized hardware or vendor-specific operating systems.

Since, potentially, a single platform may be used for multiple applications, users, and tenants, the hardware-software decoupling lowers equipment costs and energy consumption. Combined with Software Defined Networking (SDN), these service-based network architectures allow for more flexible and dynamic network management [49]. Network engineers now have more options and better control over network performance, allowing quicker and more effective use of network resources. Network softwarization also creates automation and system integration possibilities, resulting in more efficient workflows across frameworks. The network then becomes a large pool of software, storage, and computing resources shared by different actors that can be programmed to optimize different objectives.

SLAs are used in networking to formalize stakeholder relationships; for instance, an SLA might specify how much latency a given NS can tolerate. Then, Network Service Providers (NSPs) can adjust the size of their NSs to satisfy user requirements while reducing CAPEX and OPEX by enabling dynamic resource provisioning. Therefore, if we assume that the network receives a workload, this workload should be processed by using the least amount of resources. At the same time, the 6G ecosystem is expected to impose even higher requirements than those used in 5G, such as extreme-low latency, ultra-high reliability, and enhanced throughput.

The easiest way to fulfill such requirements is by overprovisioning, in other words, securing enough resources to perform well in the worst-case scenario when there is a high peak in the workload. These two ideas are contradictory since, on the one hand, NOs want to use fewer resources to save money, but on the other hand, they need to reserve more resources to serve higher peak workload. Thus, a balance between the cost of deploying the different container replicas and the quality objectives specified in the SLAs must be achieved.

In this paper, we assume a very simple yet challenging scenario where a NSP must deploy a service consisting of one containerized NF (e.g., video transcoder). Users or other services in the network can request this service by submitting processing tasks or jobs. To meet SLAs, the NSP resizes its NSs, by changing the number of the replicas of the NFs to fulfill operational and business objectives in a multi-objective setup [50]. We consider horizontal scaling instead of vertical scaling since it can be exploited by distributed applications where a workload is shared among different instances of the same application. While vertical scaling is limited to the capacity of a single server, horizontal scaling leverages the virtually infinite computing capacity in cloud environments, making it easier to deploy several instances of the same application. Additionally, horizontal scaling allows more granular control of NFs in multi-tier applications where each tier is scaled independently.

As mentioned above, the system is assumed to work in a time-slotted fashion. At the beginning of the slot, the workload, expressed in terms of jobs per unit of time, queues in front of a load balancer. If no jobs are in the queue, the workload is equally distributed among the number of active replicas. Notice that a job may incur some latency even when no queue is present since they are sequentially processed at the replica level. Otherwise, the incoming batch of jobs waits in the queue until they can be processed by one of the replicas. Each replica can process a predetermined number of jobs per time slot. Finally, a decision engine determines the number of replicas in the following slot, depending on the accumulated and the expected work to be processed. The process repeats at the next time slot. Figure 3 depicts the system described above.

4.2. Scaling as an MDP

Under these circumstances, scaling can be modeled as a decision-making problem since, in each time step, a decision about the number of replicas should be made. An MDP is a discrete-time stochastic framework that models decision-making problems. The notations used throughout this paper are summarized in Table 1. In general terms, an MDP is defined by the tuple $\langle \mathcal{S}, \mathcal{A}, P, r \rangle$ where \mathcal{S} and \mathcal{A} are the state and action spaces; $P : \mathcal{S} \times \mathcal{A} \times \mathcal{S} \rightarrow [0, 1]$ is the transition kernel, with $p(s'|s, a)$ denoting the probability of transitioning to state s' from s after action a is taken; $r : \mathcal{S} \times \mathcal{A} \times \mathcal{S} \rightarrow \mathbb{R}$ is the immediate reward obtained for performing action a , following a predetermined RFn. The policy $\pi : \mathcal{S} \rightarrow \mathcal{P}(\mathcal{A})$, is a mapping function from the state space to the space of probability distributions over the actions, with $\pi(a|s)$ denoting the probability of selecting action a in state s . The solution to an MDP is an optimal policy that maximizes the expected long-term

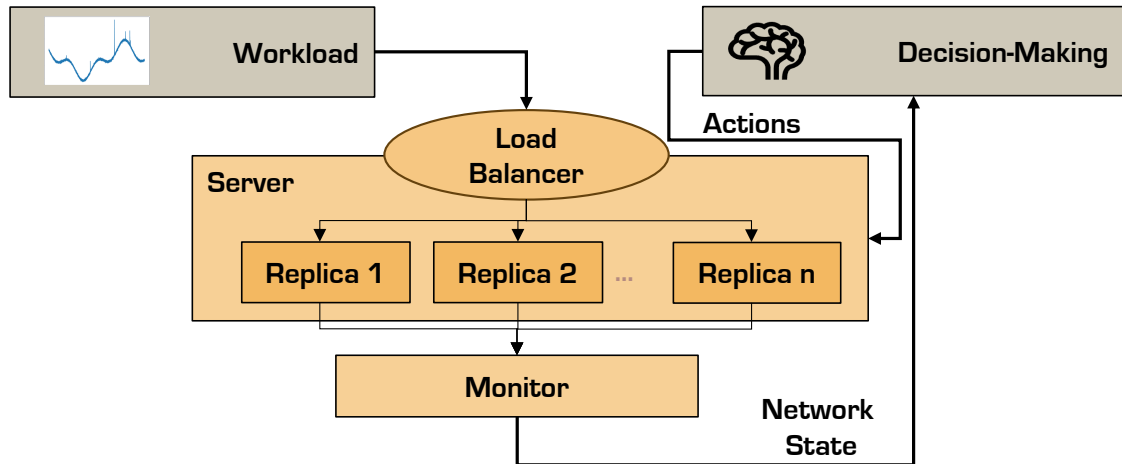


Figure 3: Simple model of the scaling problem.

reward, which is a discounted sum of immediate rewards. This optimal policy mostly uses iterative solution methods, e.g., value or policy iteration.

Modeling scaling as a MDP allows us to design the scaling solution as a closed-loop control, which leverages autonomy and adaptiveness. Following the MAPE-K, one of the most influential reference control models for autonomous and self-adaptive systems [51], a closed-loop control involves establishing a feedback system where the scaling of resources is continuously adjusted based on observed performance metrics.

As shown in Figure 4, the *Monitor* function collects data from the resources through sensors distributed over the system, constituting the state s of the system. For instance, the system can monitor factors like server load, response times, and resource utilization in cloud computing. Then, the *Analyze* function correlates the received information and creates a system model. This model allows the closed-loop control system in the *Plan* function to automatically trigger action a when deviations from optimal performance are detected, such as provisioning additional resources to meet demand or scaling down to save costs during periods of lower activity. Finally, the *Execute* function performs the planned actions over the resources. The *Knowledge* is represented by the data shared among the previous functions.

In the problem described in the subsection above, the information retrieved by the *Monitor* function composes the network state. At time step t , the state s_t is defined as a tuple $\langle v_t, c_t, d_t \rangle$ where v_t represents the number of active replicas, c_t is the mean CPU usage among the active replicas, and d_t is the processing latency from the active replicas, i.e., the peak latency introduced by processing the jobs. Based on this information, the decision-maker decides its actions. This simple model keeps the action space small by only defining three actions. Thus, a_t is a number from the set $\mathcal{A} = \{-1, 0, 1\}$, where -1 means to decrease the number of replicas by one, 1 means to increase the number of replicas by one, and 0 will maintain the same number of replicas. Only one action is allowed per time slot.

To complete the framework, the decision-maker receives a reward every time slot if its action leads towards the end goal. Notice that if the reward is only penalizing extremely high latencies, the decision-maker will take the most obvious action: to keep increasing the number of instances, disregarding the economic impact of such a decision. Therefore, one of the critical aspects in designing a solution for an MDP is the RFn definition. Depending on the RFn, different policies can be found.

5. Model Design: DRL algorithms for scaling

Once the problem has been defined, we can proceed to the next step in the design phase. Since the data for RL approaches is obtained through continuous interaction with an environment, we skip the data

Table 1: Variables used in this paper.

Variables	Description
\mathcal{S}	State space.
s, s_t	A particular state in step t .
\mathcal{A}	Action space.
a, a_t	A particular action in step t .
P	Transition Kernel.
$p(s' s, a)$	Transition probability to state s' by taking action a in state s .
r	Immediate reward.
$\pi(a s)$	Probability of selecting action a in state s .
ϵ	Tolerance range.
v_t	Number of active replicas in step t .
\bar{v}	Mean number of active replicas during a period of time.
c_t	Mean CPU usage of the active replicas in step t .
c_{tgt}	CPU utilization target.
d_t	Processing latency of the active replicas in step t .
d	Mean latency of the active replicas during a period of time.
d_{tgt}	The target latency. The maximum tolerated value $(1 + \epsilon) \cdot d_{tgt}$ cannot be surpassed.
c_{perf}	Performance cost.
w_{perf}	Importance (weight) of c_{perf} in the total cost.
c_{res}	Resource cost.
w_{res}	Importance (weight) of c_{res} in the total cost.
V'	Normalized number of replicas created by an agent.
w_v	Importance (weight) of V' in networking scoring.
D'	Normalized latency of an agent.
w_d	Importance (weight) of D' in networking scoring.

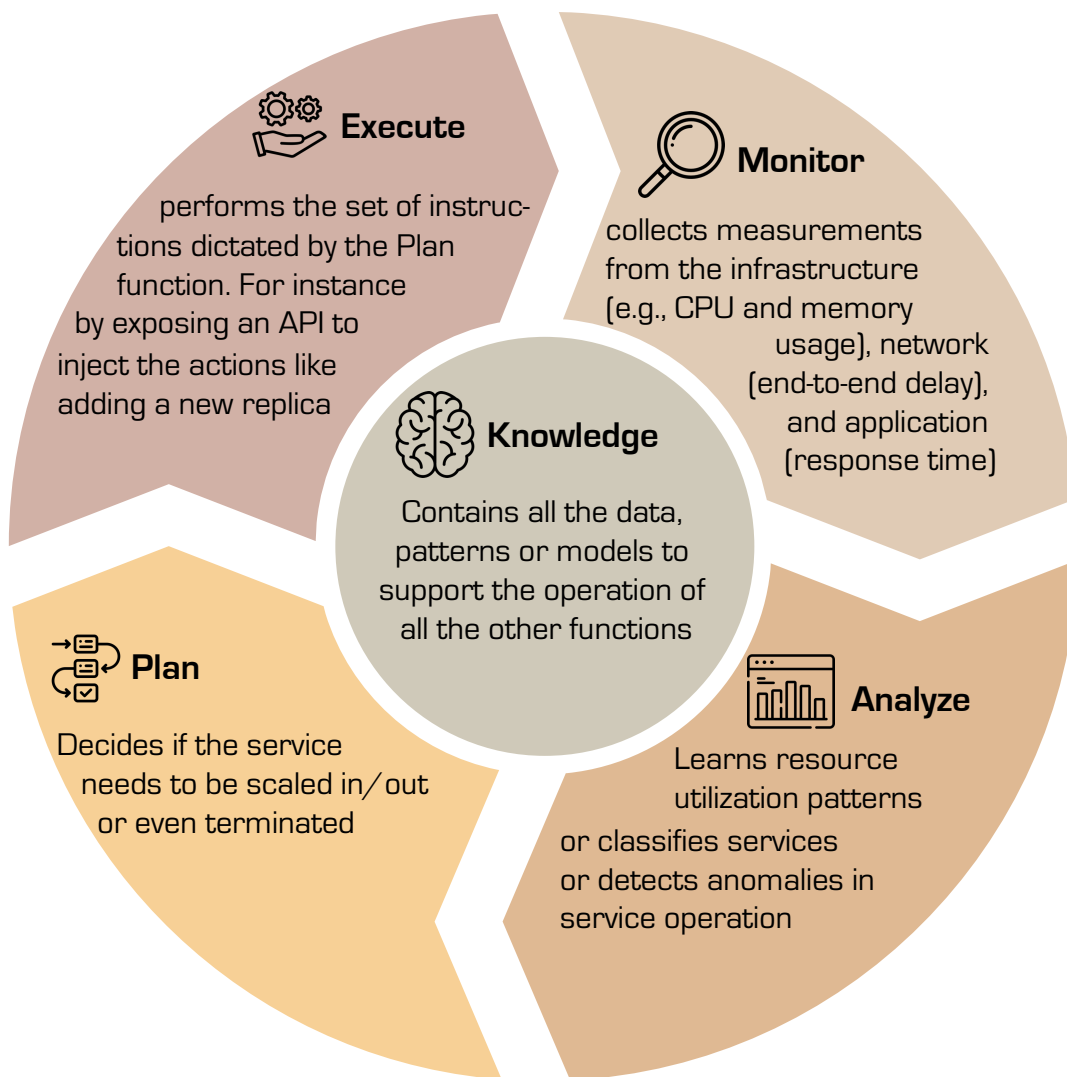


Figure 4: Closed-loop control in the scaling problem, according to the MAPE-K framework.

preparation step. Then, we can design the model that will solve the problem. This section explores the intricacies of designing DRL algorithms tailored explicitly for efficiently scaling resources. Based on the problem constraints elaborated in Section 4, we discuss the nuanced aspects of algorithmic design, elucidating key principles and methodologies essential for achieving proper lifecycle management of this type of NI in service-based architectures.

5.1. DRL algorithms tailored to the Scaling problem

RL has emerged as a powerful and versatile approach for solving MDPs, offering a robust framework to tackle a wide range of complex decision-making problems. RL’s appeal lies in its ability to address MDPs by exploring and analyzing the effects of different actions in an environment, making it well-suited for dynamic and uncertain scenarios. RL’s capacity to adapt to various environments and its capability to navigate the intricate trade-offs between exploration and exploitation makes it a compelling choice for finding optimal policies within the context of MDPs. This adaptability, coupled with its potential for achieving near-optimal solutions over time, underscores why RL stands as a prominent and effective tool for solving MDPs [52].

The most well-known RL algorithm is Q-Learning. When the state and action spaces derived from the MDP are sufficiently small, Q-Learning can store the value functions as arrays or tables [52]. In this case, the approaches can find exact solutions; that is, they can find the optimal value function and the optimal policy if they visit each state-action pair an infinite number of times [53]. Since the data coming from the *Monitor* function is typically real-valued, tabular Q-Learning lacks scalability due to the quantization of the monitored samples, making this approach impractical for scaling as the size of the tables is unpractically large. On the contrary, DRL is preferred for complex, high-dimensional, or continuous state and action spaces. Under DRL, a deep neural network approximates the value function, policy, or both. These neural networks provide the capacity to handle high-dimensional and uncountable infinite state spaces.

DRL algorithms can be classified as on-policy or off-policy. Off-policy algorithms update their policy using data generated by a different policy. This means that the agent can learn from past experiences and use data collected by any previous policy, making them more sample-efficient but potentially introducing higher variance in the learning process. On the other hand, on-policy algorithms update their policy while using the data generated by the same policy. This means that the data collected during the learning process is directly used to improve the current policy, leading to more stable but potentially less sample-efficient performance. As a result, the policy being learned is constantly changing as the agent explores the environment and gathers new experiences. Other classifications of DRL techniques are possible. We refer the reader to [54] for a detailed view of the state-of-the-art of these kinds of algorithms.

Given the properties of the scaling problem, there are two known DRL algorithms that are suitable, namely, a Deep Q-Network (DQN) [55] and Proximal Policy Optimization (PPO) [56] algorithm. DQN is a type of off-policy, value-based algorithm that combines Q-learning with deep neural networks to estimate the value of states or state-action pairs. Being a value-based algorithm, DQN learns the value of each action in a given state to later select the actions that maximize the expected reward over time. Through repeated interactions and learning from the experience replay buffer, the DQN can learn an optimal policy to perform well in complex tasks. Still, it may struggle with high-dimensional state spaces. It has been successfully applied to various tasks, including playing Atari games and controlling robotic systems [57].

On the other hand, PPO is an on-policy, policy-based algorithm based on policy gradient. Policy-based RL directly parameterizes the policy mapping states to actions without explicitly learning a value function, offering greater flexibility and robustness in exploring the action space. However, more samples may be required to converge to an optimal policy than value-based methods. PPO tries to address the limitations of previous policy gradient algorithms such as Trust Region Policy Optimization (TRPO) by striking a balance between making significant updates to the policy (to improve performance) and ensuring that the updates are not too large, which could lead to instability or catastrophic changes. PPO achieves this by updating the policy with a “clipped” objective function.

5.2. Reward Functions (RFns)

We designed three RFns to guide the agents’ learning. The goal in proposing multiple RFns is twofold. On one side, we want to highlight that the RFn definition is among the most difficult aspects in RL. Here,

we have three different RFns for the same problem, and though they seem to be logical and make sense, not all of them yield good results, as shown in Section 7. Conversely, the exploratory work performed in this study may help uncover a broader spectrum of potential solutions and can lead to more robust and adaptive learning.

5.2.1. Reward Function 1 (RFn1): Inspired from cart-pole

Contrary to most of the RL applications in networking, where the states, actions, and RFn are defined using a networking rationale, in this RFn, we map the auto-scaling problem to known applications of RL. One of the classical environments in OpenAI Gym is *Cart-Pole*,¹ where a pole is attached to a cart moving along a frictionless track. The pole is placed upright on the cart, and the goal is to balance it by applying forces to the left and right sides of the cart. Similarly, in scaling, the agent tries to guarantee a given SLA (e.g., latency) by taking discrete actions (i.e., increase, decrease, or maintain the number of replicas) that resemble the ones taken in *Cart-Pole* by applying forces to the left or the right. Consequently, the RFn is defined similarly as in the *Cart-Pole* problem. More specifically, the RFn at step t is defined as

$$r_t = \begin{cases} 1 & |d_t - d_{tgt}| < \epsilon \cdot d_{tgt} \quad \vee \\ & |c_t - c_{tgt}| < \epsilon \cdot c_{tgt} \\ 0 & |d_t - d_{tgt}| \geq \epsilon \cdot d_{tgt} \quad \vee \\ & |c_t - c_{tgt}| \geq \epsilon \cdot c_{tgt} \\ -100 & \text{if wrong behavior} \end{cases} \quad (1)$$

where d_{tgt} is the target latency as defined by the SLA and ϵ is a range of tolerance (e.g., 20%). If the RFn is only defined based on the perceived latency, the agent will take the most obvious action: to keep increasing the number of instances, disregarding the economic impact of such a decision. To keep the number of instances at an adequate level, we also reward the agent if the current CPU usage, c_t , is within a predefined range. If the CPU usage is low, probably the workload can be served using fewer replicas and vice versa. Moreover, the agent is severely penalized if it incurs in a wrong behavior, such as creating more replicas than necessary or exceeding the perceived latency beyond an allowed upper bound. Notice that the CPU utilization target, c_{tgt} , is not normally specified by the SLA and must be approximated.

5.2.2. Reward Function 2 (RFn2): A Markov Reward Process

A Markov Reward Process (MRP) is a mathematical framework used to model and study the behavior of a system that involves stochastic transitions between states and yields rewards over time. MRPs are used to formalize problems where an agent interacts with an environment, and the agent receives rewards for being in certain states. This way, MRPs could be directly applied to RL setups. A MRP is defined by mainly three concepts: the states, the transitions, and the rewards. Notice that it is not necessarily the case that the states of the MRP are the same as in the MDP.

Particularly for the scaling problem, we define two states: the process exhibits a latency above the specified threshold, or the process shows a latency below the defined threshold. The agent dictates the transitions between these two states with its actions. For example, it can be that the process is below the latency threshold, but the agent decides to remove a replica, which takes the process to the state of being above the latency threshold. Then, the algorithm designer can establish what actions led to a good outcome and which did not.

Figure 5 shows an example of such MRP. In green are depicted the actions that we consider good because they lead toward the goal we want to achieve, i.e., fulfilling the SLA with the least amount of replicas possible. In contrast, depicted in red are the actions that push us away from that goal. More specifically, for both agents, we only reward the good actions. We noticed that by using positive reinforcement, the agents could show a better performance. Then, the RFn we used was defined as follows.

¹https://www.gymnasium.dev/environments/classic_control/cart_pole/

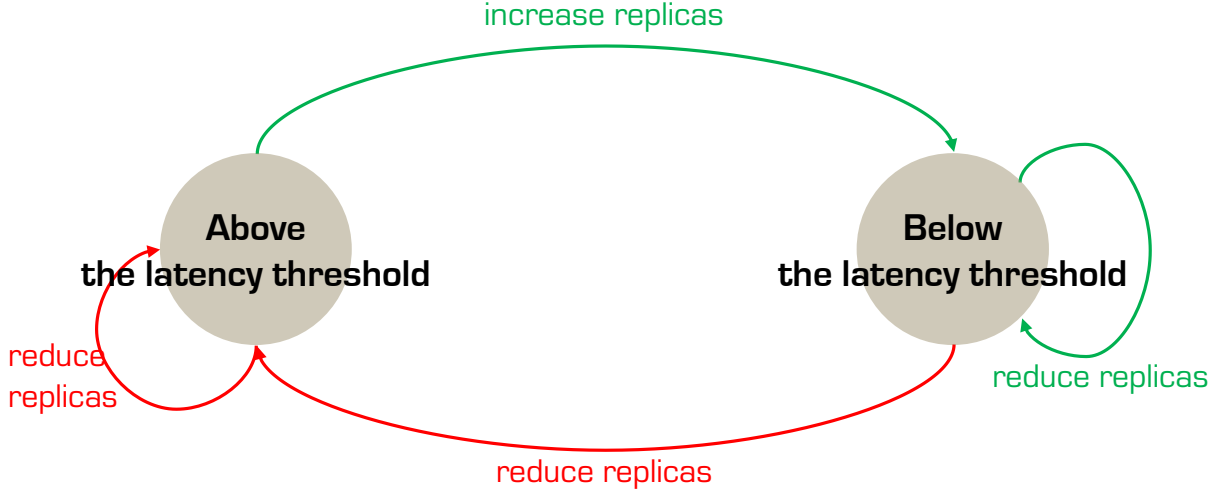


Figure 5: Markov Reward Process for auto-scaling

- If the process was in state *Above*, and the agent’s action was to increase the number of replicas, which led to the process being in the *Below* state, the agent receives a reward of 1. In this case, the agent is encouraged to increase the number of replicas only to fulfill the SLA.
- If the process was in state *Below*, and the agent’s action was to decrease the number of replicas, which led the process to keep being in the *Below* state, the agent receives a reward of 1. In this case, the agent is encouraged to use resources efficiently when the SLA is fulfilled.
- All the other combinations of states and transitions are not rewarded nor penalized.

5.2.3. Reward Function 3 (RFn3): A Multi-Objective Function

This RFn aims to fulfill the agreed SLA with the minimum amount of replicas. Therefore, in every time step, the agent pays an immediate cost depending on how good or bad the action it took is. The cost of taking action when the environment moves from one state to another can be defined as a weighted function, including the following contributions.

- If the agent cannot fulfill the SLA, it incurs a performance cost c_{perf} , with an associated w_{perf} , which is paid every time the perceived latency d exceeds a maximum tolerated latency, $(1 + \epsilon) \cdot d_{tgt}$. The cost is zero otherwise.
- If the agent must deploy a new replica, a resource cost c_{res} is paid, with an associated w_{res} ; this can be seen as a rental cost in cloud environments or the consumed energy of the replica while it is running.

These two contributions are combined into a weighted function, shown in Equation 2, where the respective non-negative weights define an optimization profile, $w_{perf} + w_{res} = 1$. The weights (w_{perf} and w_{res}) multiply an indicator function $\mathbb{1}\{\cdot\}$ that varies between 1 and -1 depending on whether or not a condition is met, as indicated in Equations 5 and 6. For instance, if the perceived latency exceeds a maximum tolerated value, the indicator function is 1; otherwise, the indicator function is 0. Conversely, if a new replica is instantiated, the indicator function is 1, or -1 if the replica is removed. Finally, the RFn is defined as the negative of the cost function.

Table 2: Optimization profiles used in RFn3.

Optimization Profile	w_{perf}	w_{res}
1	0.5	0.5
2	0.01	0.99
3	0.99	0.01

$$r = -c_{total} = -(c_{perf} + c_{res}) \quad (2)$$

$$c_{perf} = w_{perf} \cdot \mathbb{1}\{perf\} \quad (3)$$

$$c_{res} = w_{res} \cdot \mathbb{1}\{res\} \quad (4)$$

$$\mathbb{1}\{perf\} = \begin{cases} 1 & d_t > (1 + \epsilon) \cdot d_{tgt} \\ 0 & \text{otherwise} \end{cases} \quad (5)$$

$$\mathbb{1}\{res\} = \begin{cases} -1 & a = \text{remove replica} \\ 0 & a = \text{maintain replica} \\ 1 & a = \text{add replica} \end{cases} \quad (6)$$

Similar to our previous work [30], we used different optimization profiles for this RFn by assigning weights. By giving equal weights, the agent should learn policies that balance the creation of replicas while not exceeding the latency threshold. On the other hand, by assigning more weight to the resource cost, the agent should learn policies that limit the creation of replicas, disregarding the impact on latency violation. Conversely, if more weight is assigned to the performance cost, the agent should learn policies that encourage the creation of replicas to minimize the latency violation. Table 2 shows the optimization profile we used in this study.

5.3. Environment

In light of the growing amount of research involving RL algorithms in networking, creating a benchmarking environment is essential to assessing and comparing the performance of the different algorithms. To address this, we created a dedicated environment to facilitate fair and comprehensive assessments of RL algorithms for scaling. This environment is tailored to the specific challenges and characteristics of the scaling problem, with the primary objectives of providing a common ground for evaluation, promoting collaboration within the research community, and tracking the progress of RL algorithms over time. In this endeavor, we consider essential components such as the definition of different RFns, the choice of evaluation metrics, and the design of test scenarios, all of which will contribute to the effectiveness of our benchmarking framework.

One of the main components in an MDP is the environment. An environment is a process that interacts with the agent and reacts to the agent’s actions by transitioning from one state to another. In the case of scaling, the environment is the system that hosts the different replicas and allows them to process the workload.

For this evaluation, we developed *DynamicSim*, a simulator that enables the creation of edge-cloud network scenarios. This simulator is based on Simulation of Discrete Systems of All Scales (Sim-Diasca)², a general-purpose, parallel, and distributed discrete-time simulation engine for complex systems written in the Erlang language [58]. Erlang facilitates the implementation of large-scale parallel and distributed applications such as the ones tackled in networking. Erlang is a functional programming language based on the actor model, a powerful model for creating highly concurrent, distributed software.

²<https://github.com/Olivier-Boudeville-EDF/Sim-Diasca>.

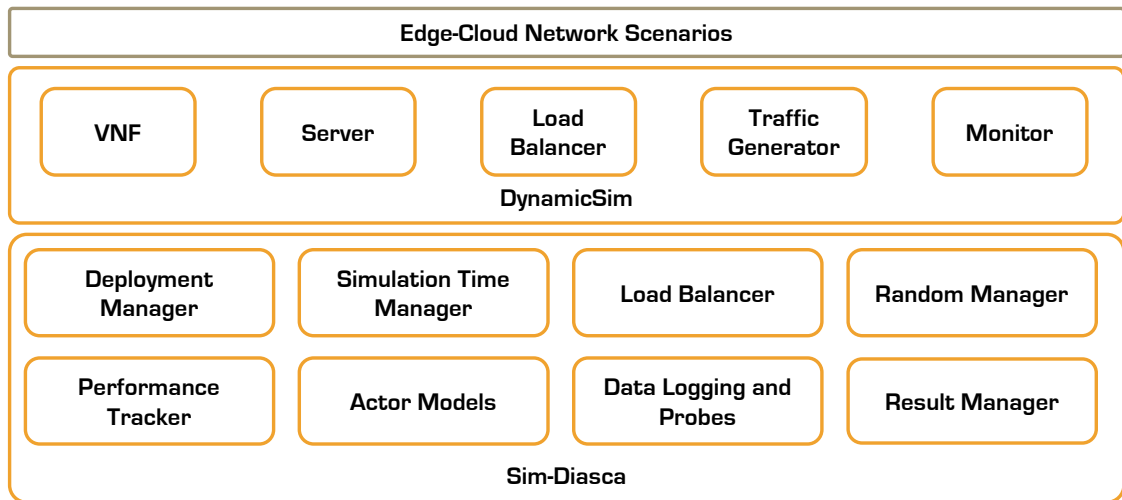


Figure 6: Architecture of Sim-Diasca [58]

Each actor in this architecture is considered a processing unit, which can communicate with other actors via asynchronous messages. Each actor stores their respective messages that are pending processing. After processing the message, an actor modifies its state, sends more messages, or makes new actors. Due to the actors' lack of shared state or resources and asynchronous communication, this paradigm significantly reduces blocking waits and race situations, two major issues with concurrent systems. Moreover, the actor model facilitates distributed software development since it makes no difference if two actors are running on the same machine or different ones.

Figure 6 shows the architecture of the simulator. Sim-Diasca (lower layer) is in charge of synchronizing the time between the actors, evolving the system state, sending and receiving messages to and from the controller (i.e., decision-making agent), and managing the results. Its built-in support for distributed simulation enables deploying simulation scenarios over multiple computers. Through the base actor model, own-defined models can be created. Therefore, *DynamicSim* defines an actor model for the replicas, the server, and the load balancer. The traffic generator and the monitor modules act as an interface between the actors in the lower layer and the high-level functions defined in Python through the sub-pub communication schema developed by ZeroMQ. Finally, we design several user-defined simulation scenarios in the topmost layer, including the one presented in Section 4.1.

However, to be able to interact with a RL agent, *DynamicSim* should follow the OpenAI Gym [18] interfaces. Such interfaces communicate the states, actions, and rewards, providing an abstraction layer between the agent and the environment. In this manner, the agent is unaware of how the environment goes from one state to another, and conversely, the environment is unaware of how the agent makes decisions. The interfaces were created using Stable-Baselines3 (SB3) custom environments, which inherit the methods from Gym Class that provide that abstraction layer. Thus, in each interaction (or step), the agent chooses an action according to a policy and receives the following state from the simulator. The agent is rewarded or penalized based on the RFn depending on the received state. This process is repeated until the agent converges to a policy that maximizes the expected reward in the long term.

At the level of the simulator, an initial set of actors is generated based on the defined simulation scenario in Sim-Diasca. In a simulation scenario, the duration of a step is user-defined. Within a step, the actors simulate its functionality, representing the work done in such a duration. After each actor finishes its simulated work, the system's state is gathered and sent to the agent, the time manager increases the step by one, and the simulation goes to the next step.

The initial scenario consists of a server with two replicas and a load balancer between them. The load balancer evenly divides the incoming workload among the created replicas. The system state at step t is

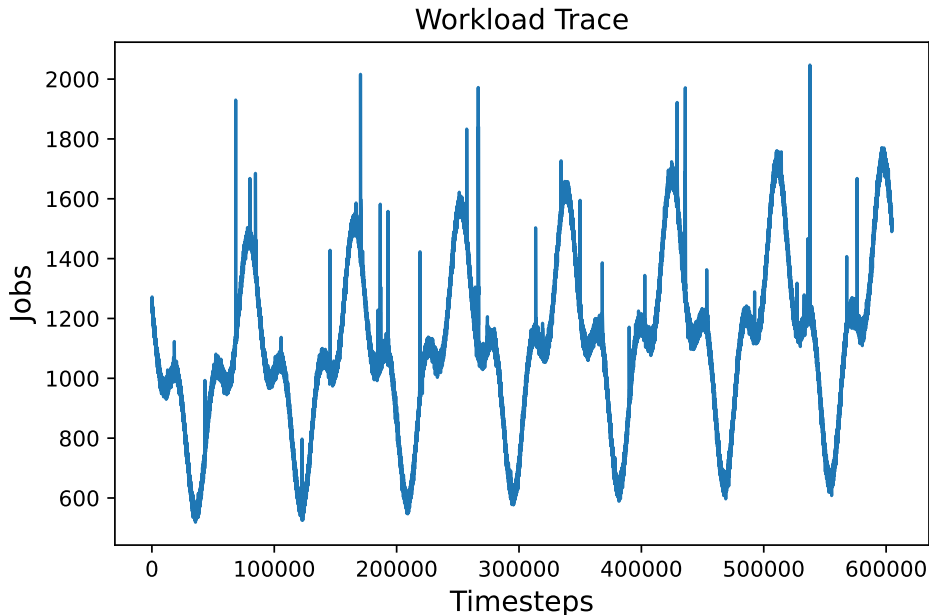


Figure 7: Complete workload trace

defined as $s_t = \langle v_t, c_t, d_t \rangle$, as explained in Section 4.1. Notice that d_t and c_t are real variables, while v_t is an integer variable, which poses the scaling problem into the continuous space. The latency is reported since we need to guarantee that each replica can fulfill the QoS requirement.

Similarly, at step t , the agent takes an action $a_t = -1, 0, 1$, where $a_t = 1$ increases the number of replicas by one, $a_t = -1$ decreases the number of replicas by one, while $a_t = 0$ keeps the number of replicas intact. However, it takes at least one slot to boot or to shut down a replica, depending on the algorithm’s decision. No job can be assigned to that particular replica during the boot time. Similarly, the replica resources are released during the shutdown time once its pending jobs are processed.

The traffic generator produces a workload following a known pattern in data centers, as shown in Figure 7. Generally, the traffic to a data center is low at night and peaks during working hours. This pattern repeats more or less during the weekday. For more details about how this workload is generated, we refer the reader to [29]. Notice that the workload replicates a dynamic and varying pattern that contains long-term and short-term fluctuations due to sudden changes. The short-term fluctuations are particularly hard to detect in traditional scaling mechanisms since the number of replicas is calculated based on worst-case estimates that do not include such variations. Although synthetic workloads may not fully represent the real incoming traffic, they are suitable for controlled experimentation.

The simulator and the abstraction layer are publicly available³ since it is within our objectives to promote openness and reproducibility of RL algorithms in the networking community, which is fundamental to benchmark ML algorithms in networking.

6. Training, validating, and selecting DRL algorithms for scaling: A methodology

In the previous sections, we detailed the influence of scaling computing resources in service-based architectures on system requirements, shaping the learning objectives for autonomous agents (cf. Section 4). Building upon these requirements, Section 5 delved into the algorithmic and environmental design underpinning the realization of autonomic control. Aligned with the infinity model, this section focuses on the

³We are currently working with the legal department at our Lab to make a public version complying with our policy of Open Data. The benchmark will be released before the publication of the manuscript.

development phase. Assuming the availability of multiple RL models for deployment, we incorporate best practices for algorithm comparison and selection, thereby expanding current MLOps frameworks.

6.1. Training

Once the appropriate RL algorithms and RFns tailored to the problem have been selected, the next step in their lifecycle is to develop the autonomous agent. This is commonly known as training. Following the recommendations from the O-RAN alliance, RL algorithms should be trained offline [16]. Offline training in networking can be performed in a NDT [46], where the outcomes of the untrained agents can be safely injected without compromising the stability of the production network [6]. The environment of Section 5.3 can serve as a NDT for the proposed use case.

A major challenge in the RL community is that minor implementation details can considerably impact performance, sometimes surpassing the disparity between various algorithms [47]. Ensuring the reliability of implementations employed as experimental baselines is paramount. Otherwise, comparing novel algorithms to unreliable baselines may result in inflated estimates of performance enhancements. Thus, standard, open-source frameworks that provide reliable implementations of RL algorithms are recommended [17, 59].

Regarding the implementation of the algorithms presented in Section 5.1, for this study, we use stable baselines, a popular framework that provides a set of reliable implementations of RL algorithms in PyTorch⁴. We use the default architecture and default hyper-parameters given by stable baselines for both algorithms. Both algorithms use two fully connected networks with 64 units per layer. While actor and critic are shared for PPO to reduce computation, DQN has separate feature extractors, one for the actor and one for the critic since the best performance is obtained with this configuration.

Additionally, since RL’s reproducibility can be far more difficult than expected [36, 35], given their random initialization of the parameters, among others, Colas et al. [60, 61] suggest evaluating several seeds of DRL algorithms in an offline manner. In this offline evaluation, the algorithm performance after training is independently assessed, usually using a deterministic version of the current policy. We call an *agent* an algorithm - RFn - seed combination.

Consequently, to compare the performance of the different RL algorithms, we follow the guidelines suggested by Colas et al. [60, 61]. In their paper, the authors suggest (i) obtaining the measure of performance of every agent to plot the learning curves of the algorithms, (ii) performing statistical difference testing, (iii) comparing the full learning curves not only comparing the final performances of the two algorithms after t steps in the environment.

Taking those recommendations into account, we extend the current methodological proposals for lifecycle management of RL applications in service-based architectures to support algorithmic comparison and selection. We summarize this extension into the methodology shown in Figure 8.

At least five different agents should be implemented initially. Each agent is trained using episodes, where an episode is defined as the number of steps until the simulation must be restarted or a maximum number of steps is reached. Accordingly, we determined two situations where an episode is terminated: when the agent creates more replicas than needed or lets the latency go above an inadmissible threshold. These two situations represent an undesired agent behavior and must be penalized. In such situations, the episode ends, the agent receives -100 of reward, and the simulation is restarted. After the simulation is restarted, the initial scenario is again deployed.

Assuming that what happens in an actual second in every step is simulated, we chose one-hour episodes. Thus, the maximum number of steps is 3600. Notice that the episode length may vary during training since, at the beginning of the training, the agent is expected to take random actions, which can easily lead to episode termination due to undesired behavior. After the agent is trained during N episodes, we freeze its policy and evaluate it during V episodes. Following the logic of SL approaches, we split the workload trace into two, one for training and another for evaluation, aiming to test the generalization capabilities of the algorithms to unseen data. The training trace uses the workload’s first 432×10^3 values (i.e., first 5 days), while the evaluation trace uses the last 172.8×10^3 values (i.e., the last 2 days). Training and evaluating the agent is considered an epoch; we repeat the process during E epochs.

⁴<https://pytorch.org/>

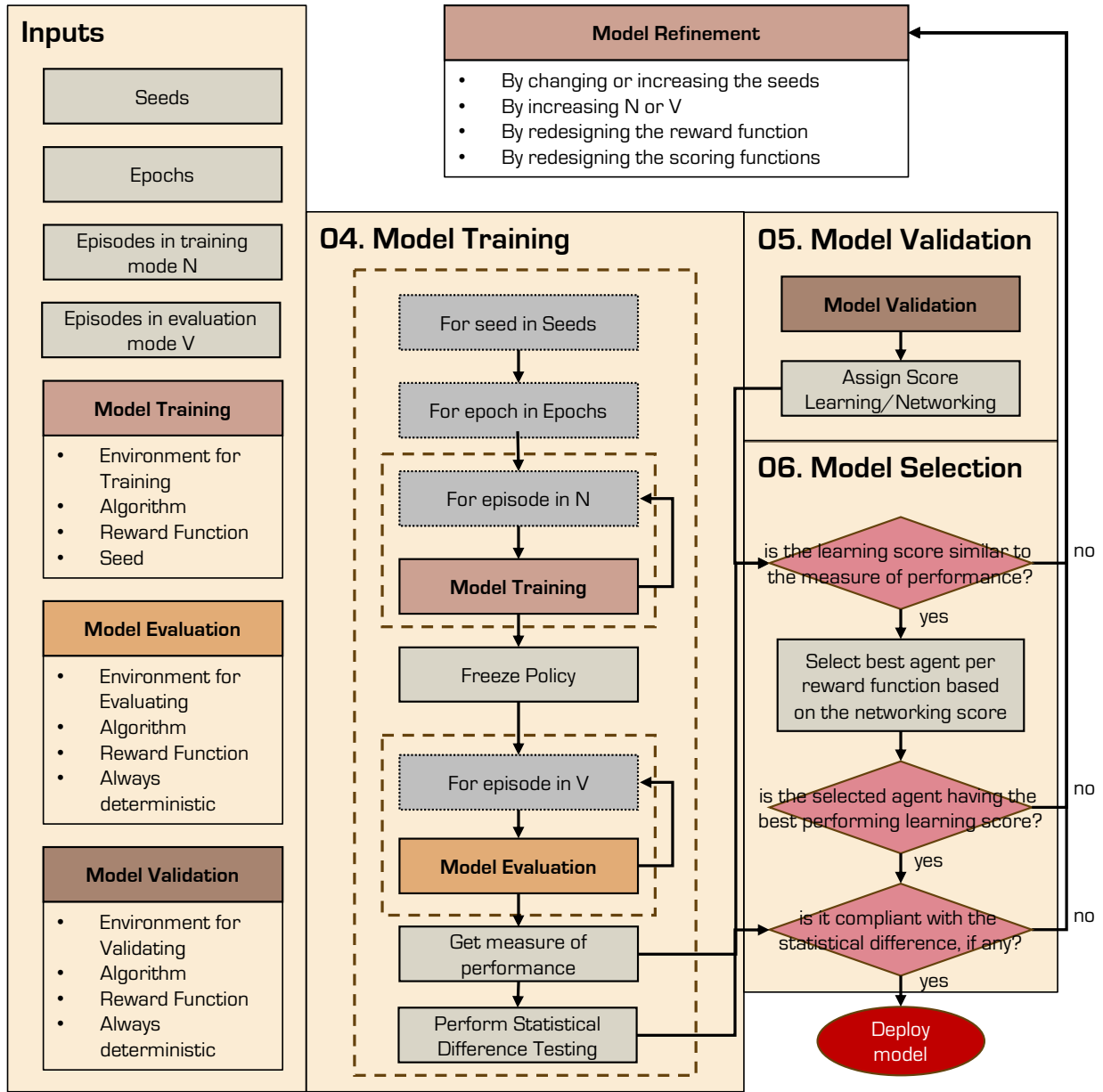


Figure 8: Proposed Methodology

Table 3: Parameters used in the experimental evaluation.

Steps per episode	3600
Episodes in training mode N	24
Episodes in evaluation mode V	12
Epochs E	10
d_{tgt}	20 ms
c_{tgt}	75%
ϵ	20%

Table 4: Minimum and Maximum reward possible in each of the reward functions.

Reward Function	Min	Max
RF1	0	3600
RF2	0	3600
RF3.1	-3600	1800
RF3.2	-3600	3564
RF3.3	-3600	36

Generally, the values of N , V , and E should be selected by trading off training time and the agent’s performance. The agent’s performance should be evaluated as soon as possible, which implies selecting a lower training time, i.e., lower N , but ensuring enough training is reflected in improving the agent’s behavior. Moreover, a larger V gives a better estimation of the true agent’s performance but, at the same time, slows down the training. Following this trade-off, we selected the values for N , V , and E for all RFns and RL algorithm combinations. The values are shown in Table 3.

At the end of an evaluation episode, we record the accumulated reward of the episode. Then, the performance per epoch is the average earned reward over the V episodes. To provide a fair comparison of the performance of the algorithms among the different RFns, all the RFns must be in the same range. Unfortunately, that is not true for the proposed RFns. However, a minimum and a maximum achievable reward can be calculated for every agent, depending on the episode duration.

Suppose an agent makes good decisions to avoid falling into episode termination cases. In that case, the maximum reward possible is the duration of a full episode times the maximum reward. A similar analysis can be done with the minimum achievable reward. Table 4 shows the range variation in each RFn, where the underscore in RFn3 indicates the optimization profile, c.f., Table 2. Having the minimum and maximum range of the reward, we apply a min-max scaler so the agents’ performance falls within the same range.

Once each agent’s and run’s performance was calculated, we performed statistical difference testing as a main way to compare their performance. In particular, we completed the Welch t-test on the data since it was more robust than other tests to the violation of their assumptions [61].

6.2. Validation

Once trained and evaluated, the performance of all the scalers is assessed. This performance can be evaluated from two perspectives: how well the agent learns and how well the agent performs the task at hand. For this purpose, we tested the learned policy in deterministic mode after the E epochs of training by letting the agent run a validation episode of 172.8×10^3 steps. We gathered the accumulated reward the agents received at the end of the validation episode and the main statistical figures of the number of created replicas and the latency. Depending on the obtained values, we score all the agents using Equations 7 and 8.

$$\text{score learning} = \frac{\text{normalized accumulated reward}}{\text{normalized episode length}} \quad (7)$$

Equation 7 scores the agents regarding the learning perspective. The episode termination cases should be avoided if the agent is well-trained. If these cases do not occur, the agent maintains the simulation running, and the episode length is the largest it could be, i.e., 172.8×10^3 steps. Then, using a min-max scaler, the normalized length of a testing episode should be 1, and the score should be approximately the same as the normalized reward achieved during training (see the y-axis of Figure 9). Suppose the agent falls into the episode termination cases. In that case, the validation episode is finalized before time, where the normalized episode length is lower than one, forcing the score to be higher than one. In this case, the agent can be discarded since it is unacceptable.

$$\text{score networking} = w_v \cdot V' + w_d \cdot D' \quad (8)$$

$$V' = 1 - \frac{\bar{v} - \text{min}}{\text{max} - \text{min}} \quad (9)$$

$$D' = \frac{\bar{d}}{\text{max}} \quad (10)$$

Equation 8 scores the agents regarding the networking perspective in terms of the number of created replicas and the fulfillment of the SLA expressed in terms of the processing latency. The goal of a scaler is to fulfill the SLA with the minimum number of replicas needed. Then, to compare how an agent performs over the remaining agents, we need also to apply normalization. For the number of replicas, we use min-max normalization as expressed in Equation 9, where \bar{v} is the average number of replicas created during the validation episode, min , and max are the minimum and the maximum values of all the created agents. In this case, we applied an inverse normalization since the min-max normalization will return values close to zero when \bar{v} is close to the minimum.

Similarly, Equation 10 normalizes the latency. By using only the maximum latency value, Equation 10 is able to identify how far this maximum is from its mean value. The closer to one, the distribution is more centered around the mean, while the closer to zero, the distribution presents a right-hand side tail. This type of normalization is handy for detecting extreme peak values in the latency distribution [62], which should be avoided in mission-critical applications, for instance. Notice that, while the min , max in the previous equation should select the minimum (or maximum) between all the created agents, the max in Equation 10 corresponds to the maximum latency value of each agent during the validation episode. This value is associated with the latency distribution of the agent itself, and therefore it is irrelevant to compare it against other agents.

Being V' the normalized value of the replicas created by a given agent and D' the normalized latency of a given agent, Equation 8 tries to find a balance between the two main objectives of the scaler. w_v and w_d are weights used to tune which of the two criteria is more important to the NSP. Moreover, the equations are chosen depending on the service type that the NF is providing. For instance, if the application allows the users to experiment some extreme latency issues, then Equation 10 could be replaced by another equation, e.g., \bar{d}/d_{tgt} measures how far are the mean latency values from the target. After all the agents have been scored, model selection can start.

6.3. Selection

Model selection is a filtering process in which all the agents that were not able to perform in a plausible way during the previous two stages are ruled out. The first step in this process is to discard all the agents whose learning score is not similar to the measure of performance obtained during the training. As explained above, a well-trained agent is able to maintain the running of the validation episode; if this is not the case, the learning score will be higher than the measure of performance, indicating a possible outlier. Such agents should undergo model refinement, by, e.g., changing the seed. We filter first by the learning score since an ill-trained agent is most likely to have a poor performance in the scaling task.

Then, by using the networking score, we select the best scoring agent per reward function. Ultimately, the agent's true performance is given in terms of the networking KPIs and not the reward the agent achieves during training. The chosen agent must satisfy two criteria: firstly, its learning score should rank among the highest within its respective RFn; secondly, if there exists statistical evidence demonstrating higher performance of one algorithm over another, the highest-performing agent should be trained using the algorithm proven to be more effective. If at least one of the criteria is met, the agent with the highest learning score should be deployed. In case none of the criteria is met, the agents should undergo model refinement, by either increasing the number of agent-environment interactions or by redesigning the RFn.

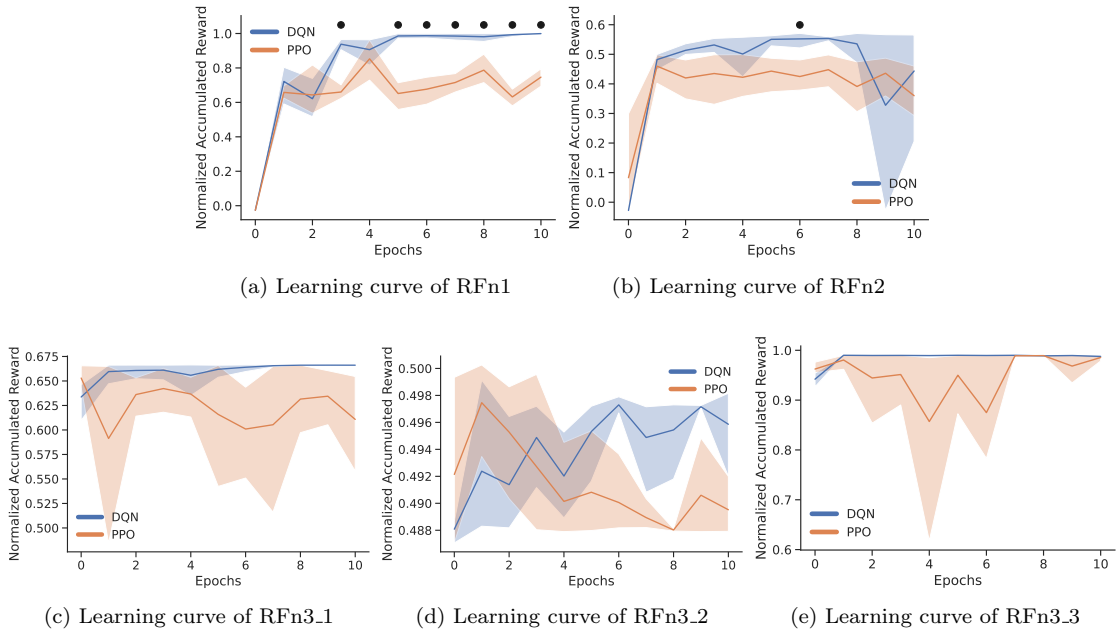


Figure 9: Learning curves, with error shades and black dots indicating significant statistical difference when present.

7. Experimental evaluation

This section presents the experimental evaluation of the two DRL algorithms and the associated RFns. Through a systematic assessment, we aim to elucidate the impact of these algorithmic and RFn choices on the learning dynamics, convergence speed, and overall effectiveness of our proposed RL methodologies. The experiments are designed to provide insightful comparisons, shedding light on the strengths and limitations of each algorithm and offering a comprehensive understanding of their behavior. This empirical analysis validates our contributions and adds to the broader discourse on designing and optimizing RL algorithms for real-world applications.

7.1. Training performance

Using the procedure described in Section 6.1, we trained and validated the algorithms of Section 5.1 using the RFns described in Section 5.2. Figure 9 shows the learning curves, with 80% error percentile and black dots indicating statistical significance when applicable for all RFns. The agents were also evaluated before training to see how much improvement that learning brings. This is plotted as epoch 0.

As it can be observed from the figure, only RFn1 shows consistent statistical difference across the epochs, where the DQN performs better than the PPO. Unfortunately, we cannot draw any conclusions for the remaining RFns; this may be due to the requirement for additional data. More data can be gathered using two different methods. On the one hand, having more seeds will enable averaging more trials, yielding a more reliable algorithm performance metric [60]. On the other hand, for some cases, e.g., Figures 9c, 9d, 9e, it is noticeable that the algorithms, especially the PPO, have not yet converged to a stable value of the reward. More training epochs can help the algorithm reach convergence in these cases.

Notice, however, that when we talk about convergence, we do not talk about the algorithm converging to an optimal policy but to a stable reward value, which a sub-optimal policy can produce. Regarding the convergence to an optimal policy, it is known that DRL approaches are sample inefficient [63] and that, for instance, Q-learning algorithms are guaranteed to converge in the limit, when each state-action pair is visited infinitely often [53]. Some strategies have been incorporated in several state-of-the-art algorithms, such as

Table 5: Learning score of all the individual runs. In red are highlighted the cases where the agents terminated the validation episode before time.

	DQN					PPO				
	Run 1	Run 2	Run 3	Run 4	Run 5	Run 1	Run 2	Run 3	Run 4	Run 5
RFn1	0.9971	0.9999	0.998	0.9999	0.9999	0.7462	0.7427	0.6765	0.6976	0.7529
RFn2	0.5662	0.5565	0.5521	0.5629	0.5598	0.3777	0.3784	0.3781	0.3784	0.3852
RFn3_1	0.6666	0.6666	0.6666	0.6666	0.6666	246.7	0.6581	1.522	0.6567	0.6588
RFn3_2	0.4975	22.28	0.4975	0.4975	0.4975	1.181	768.0	340.3	594.4	22.18
RFn3_3	43.92	0.9901	0.9901	0.9901	0.9901	0.9901	0.9901	0.984	0.9894	0.989

Table 6: Networking score of all the individual runs. The red dash identifies the agents disregarded in the previous stage, while in green are shown the best-performing agents per RFn.

	DQN					PPO				
	Run 1	Run 2	Run 3	Run 4	Run 5	Run 1	Run 2	Run 3	Run 4	Run 5
RFn1	0.4142	0.4467	0.4166	0.4591	0.4567	0.4525	0.4519	0.4496	0.4444	0.4513
RFn2	0.5219	0.5225	0.5265	0.4472	0.4455	0.4867	0.4968	0.4883	0.5005	0.4931
RFn3_1	0.4499	0.5062	0.4999	0.4774	0.4736	-	0.3886	-	0.4193	0.3894
RFn3_2	0.8695	-	0.7842	0.8863	0.8873	-	-	-	-	-
RFn3_3	-	0.3026	0.2577	0.3462	0.3977	0.4416	0.4630	0.4190	0.4289	0.3844

using a ε -greedy policy where $\varepsilon > 0$ or by using a learning rate close to zero. However, in practice, DRL algorithms require millions of samples to achieve good and stable performance depending on the task [56, 55].

In our problem, we trained and evaluated each algorithm during N and V episodes (see Table 3), where each episode consists, in the best case, of 3600 samples or interactions. Then, we have $3600 \times V \times E = 432 \times 10^3$ samples or $3600 \times (N + V) \times E = 1296 \times 10^3$ samples, if we consider the training interactions. The number of samples we used is lower than those conventionally used in RL. Nevertheless, both DRL algorithms are able to stabilize when using RFn1 (Figure 9a), and to some extent, using RFn2 (Figure 9b), while the DQN is also able to stabilize using RFn3_1 (Figure 9c) and RFn3_3 (Figure 9e).

The value around each agent stabilizes differs from RFn to RFn. This is because of how often they achieve a reward in their trajectory. In RL, a trajectory refers to a sequence of states, actions, and rewards an agent experiences while interacting with an environment over a certain period. Trajectories are fundamental to RL as they are used to learn and update the agent’s policy or value function, enabling it to make better decisions based on the cumulative experience gained during these trajectories. In the following, we will look closely at each RFn, and via the results from the testing phase, we will analyze how each RFn influences the agent’s behavior in the number of created replicas and the latency control.

7.2. Validation performance

As mentioned in Section 6.2, we run each agent in a validation episode. The scores of each run are shown in Tables 5, and 6. Regarding the learning score, we observe in Table 5, the cases where this score is above 1, highlighted in red. Such cases, are immediately discarded and are not scored using Equation 8. According to the methodology introduced in Section 6 (see Figure 8), such agents can be replaced by others by changing the seed, for instance. Besides that fact, for most cases, the learning score corresponds to the stabilizing value of the normalized reward in their learning curves, as shown in Figure 9. In general, the learning score of the agents per RFn and algorithm is similar, which leads us to think that the algorithms can find an akin policy independently of their weight initialization.

Regarding the networking performance, as depicted in Table 6, agents that were eliminated in the previous stage are denoted with a red dash, while those with the highest scores per RFn are highlighted in green. Similar to Table 5, scoring is consistent among agents trained with the same RFn. However, our two-step approach, as outlined in our methodology, enables the identification of the most suitable model for deployment.

Table 7: Main Statistical values of Run 4 and 1 of the DQN using RFn1.

	Replicas		Latency	
	Run 4	Run 1	Run 4	Run 1
mean	5.0771	5.1889	0.0089	0.0088
std	1.1276	1.2358	0.0004	0.0011
min	2.0000	1.0000	0.0058	0.0058
25%	5.0000	4.0000	0.0087	0.0086
50%	5.0000	5.0000	0.0089	0.0087
75%	6.0000	6.0000	0.0090	0.0090
max	9.0000	9.0000	0.0612	0.1440

Table 8: Main Statistical values of Run 1 and 4 of the PPO using RFn1.

	Replicas		Latency	
	Run 1	Run 4	Run 1	Run 4
mean	5.1234	5.5248	0.0085	0.0088
std	0.5913	0.4996	0.0012	0.0012
min	2.0000	2.0000	0.0058	0.0058
25%	5.0000	5.0000	0.0081	0.0085
50%	5.0000	6.0000	0.0084	0.0089
75%	5.0000	6.0000	0.0090	0.0091
max	6.0000	6.0000	0.0608	0.0656

For instance, suppose we adhere to the conventional method of selecting the agent with the highest accumulated reward. In that scenario, agents 2, 4, and 5 of the DQN utilizing RFn1 could all be considered viable options. Nevertheless, upon closer examination of their scores, it becomes apparent that agent 2 slightly underperforms compared to the others. Furthermore, as illustrated in Table 6, PPO agents demonstrate better-than-anticipated performance, contrary to expectations based solely on their learning scores.

Combining both tables reveals that, in certain instances, assumptions based on learning scores align with evidence from networking scores. For example, agents trained with RFn1 consistently outperform PPO agents in both learning and networking. Similar trends are observed in RFn2. In the case of RFn3_1, although both algorithms exhibit similar learning performance, DQN demonstrates clear superiority over PPO in networking. Conversely, in RFn3_3, while all agents exhibit similar learning scores, networking scores indicate better performance by PPO agents for this specific function. In the following section, we look more closely at the behavior of the agents per RFn, including the best-performing ones.

7.3. Selection

According to the proposed methodology, the best-performing agents are (i) DQN *Run 4* using RFn1, (ii) DQN *Run 3* using RFn2, (iii) DQN *Run 2* using RFn3_1, (iv) DQN *Run 5* using RFn3_2, and (v) PPO *Run 2* using RFn3_3. In the following subsections, we analyze the agents' behavior per RFn.

7.3.1. Analysis of the behavior of the agents using RFn1

This function rewards the agent if the monitored latency d_t or CPU usage c_t is between an upper and a lower bound of a target latency d_{tgt} and CPU usage c_{tgt} . If the target CPU usage and latency values are known, upper and lower bounds can be easily determined by setting a tolerance range. The target latency can be established by the SLA while the CPU target needs to be calculated according to operational needs.

For this RFn, we assume a target latency of 20ms and a CPU usage target of 75% with a tolerance of 20%, as indicated in Table 3. That means, if d_t is between 16 - 24ms or the c_t is between 60 - 90%, the agent is rewarded. Notice that we do not penalize our agents since we do not want to prevent the agents

Table 9: Main Statistical values of Run 3 and 5 of the DQN using RFn2.

	Replicas		Latency	
	Run 3	Run 5	Run 3	Run 5
mean	5.1839	5.3033	0.0170	0.0187
std	2.0269	2.2333	0.0110	0.0128
min	1.0000	1.0000	0.0058	0.0058
25%	4.0000	3.0000	0.0087	0.0086
50%	5.0000	5.0000	0.0119	0.0120
75%	6.0000	7.0000	0.0215	0.0261
max	14.0000	19.0000	0.0596	0.1440

Table 10: Main Statistical values of Run 4 and 1 of the PPO using RFn2.

	Replicas		Latency	
	Run 4	Run 1	Run 4	Run 1
mean	4.5307	4.4914	0.0240	0.0261
std	0.8132	0.8377	0.0332	0.0347
min	2.0000	2.0000	0.0058	0.0058
25%	4.0000	4.0000	0.0091	0.0092
50%	5.0000	4.0000	0.0094	0.0094
75%	5.0000	5.0000	0.0114	0.0117
max	7.0000	7.0000	0.1314	0.1341

from exploring different actions. Figure 9a shows that only RFn1 provides statistical evidence to support the fact that DQN agents are behaving better than the PPO ones.

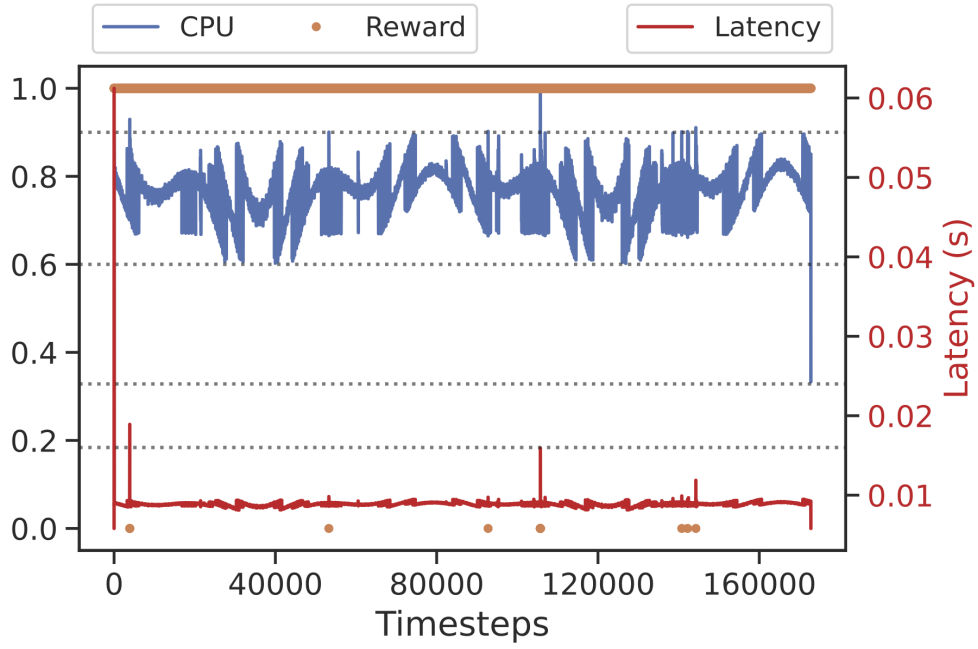
Tables 7 and 8 detail statistical metrics for replica creation and latency among different agents, including the top-performing DQN (*Run 4*), the underperforming DQN (*Run 1*), and two PPO agents with intermediate scores. DQN agents generally create more replicas to maintain low latency, with DQN *Run 4* excelling in latency control by minimizing replica creation while achieving the lowest maximum latency. Conversely, DQN *Run 1* struggles with latency control in 25% of cases, leading to a significant penalty in networking score. Although the PPO agents achieve comparable scores to DQN *Run 4*, their higher maximum latency and average replica creation slightly diminish their overall performance.

Despite their lower learning scores, the PPO agents demonstrate performance comparable to DQN agents with higher learning scores. Figure 10 showcases the top-performing DQN agent (*Run 4*) and PPO agent (*Run 4*), which has one of the lowest learning scores for RFn1. In the graph, the orange line represents the reward achieved by the agent at each step, while the blue and red lines denote the average CPU usage and peak latency of created replicas, respectively. Horizontal black dotted lines indicate CPU and latency bounds.

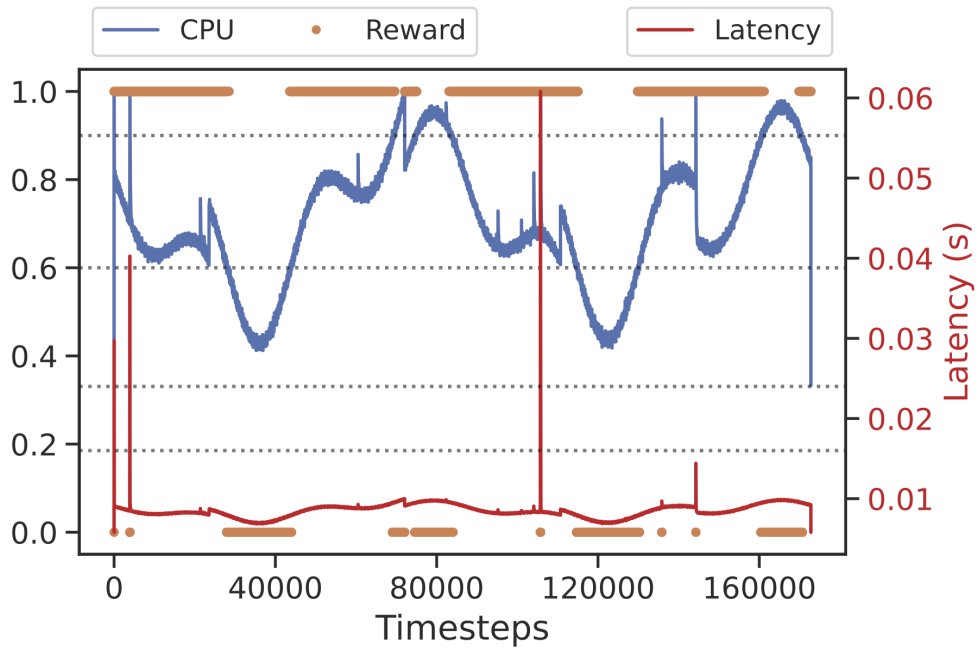
Notably, the DQN agent consistently receives rewards at each step, while the PPO agent struggles, particularly during periods of low or high workload. The success of DQN agents lies in their superior control of CPU usage. By adjusting the number of replicas, both DQN and PPO agents effectively manage latency, often keeping it below the lower bound. However, controlling the CPU usage has a smoother effect on the required number of replicas than the peak latency.

7.3.2. Analysis of the behavior of the agents using RFn2

We assume the same latency target for this RFn as for RFn1, 20ms. Consequently, the *Above* state is defined as d_t above the latency target, while the *Below* state is defined as d_t below that target. Some of the trajectories of the agents using RFn2 reflect that once an agent is below the latency, it reduces the number of replicas, so it slightly goes above the latency. Being there, the agent increases the number of replicas so it can receive the reward. This behavior is repeated several times during a trajectory, allowing the agent to



(a) Run 4 of DQN



(b) Run 4 of PPO

Figure 10: Different agent behavior using RFn1. In blue is the CPU usage; in orange is the achieved reward per step; in red is the latency. The black-dotted line shows the respective thresholds

Table 11: Main Statistical values for the best- and worst-performing agents in RFn3.1

	Replicas		Latency	
	DQN	PPO	DQN	PPO
	Run 2	Run 2	Run 2	Run2
mean	5.8264	5.3298	0.0083	0.0188
std	1.1600	0.4704	0.0004	0.0795
min	2.0000	2.0000	0.0058	0.0058
25%	5.0000	5.0000	0.0080	0.0082
50%	6.0000	5.0000	0.0084	0.0088
75%	7.0000	6.0000	0.0086	0.0092
max	9.0000	6.0000	0.0297	1.0540

Table 12: Main Statistical values for the best- and worst-performing agents in RFn3.2

	Replicas		Latency	
	DQN	DQN	DQN	DQN
	Run 5	Run 3	Run 5	Run 3
mean	4.0099	4.0693	1.8218	1.4444
std	1.0661	1.0050	0.0594	0.5496
min	1.0000	1.0000	0.0058	0.0058
25%	3.0000	4.0000	1.8190	0.6975
50%	4.0000	4.0000	1.8221	1.7559
75%	5.0000	5.0000	1.8267	1.8124
max	8.0000	7.0000	1.9345	1.9549

receive a reward every 2 or 3 steps with the side effect of occasionally trespassing the latency target. Since the agents cannot be rewarded in every step, only a certain combination of actions will produce a reward, which can be considered a sparse RFn. However, finding a suitable policy within a reasonable time is more difficult in a sparse reward setting than in a dense one [64]. The RFn’s sparsity is also why the learning score of the DQN and PPO agents is lower than their counterparts using RFn1.

Figure 9b, and Tables 5 and 6, suggest that DQN agents perform subtly better than the PPO ones. Still, this is not the case for every epoch, especially towards the final ones where the DQN agents seem to suffer catastrophic forgetting. Regarding the score, Table 5 shows that the agents are also behaving similarly in this RFn. That means that the agents are finding similar policies independently of the initialization of their parameters.

We show each algorithm’s best and worst-performing agents as in the first RFn, according to the networking score. In particular, we compare *Run 3* and *Run 5* from the DQN and *Run 4* and *Run 1* from the PPO as the best and worst-performing, respectively. The results are shown in Tables 9 and 10. The DQN agent of *Run 3* is able to achieve a better score thanks to how well it manages the latency. Unfortunately, the networking score does not measure the maximum of created replicas in both the DQN and the PPO agents and focuses more on the maximum latency instead.

More than 25% of the time, DQN agents exceed the latency target, whereas PPO agents surpass this threshold less than 25% of the time. Although PPO agents experience high latency peaks for brief periods, resulting in a lower score, their behavior in this RFn is particularly noteworthy. PPO agents adjust replica numbers to transition between states, initially increasing replicas to reach the *Below* state, then reducing them to obtain rewards, before transitioning back to the *Above* state. This cyclic process leads to a gradual increase in achieved rewards over time. Conversely, DQN agents employ a similar strategy but exploit the absence of penalties for creating surplus replicas, remaining in the *Below* state with excess replicas to increase the likelihood of reward acquisition. However, both agent types struggle to meet SLA requirements, with approximately 20% of the time spent in violation, indicating the need for a more refined RFn design.

Table 13: Main Statistical values for the best- and worst-performing agents in RFn3.3

	Replicas		Latency	
	PPO	DQN	PPO	DQN
	Run 2	Run 3	Run 2	Run 3
mean	6.9999	13.4588	0.0077	0.0062
std	0.0215	1.4178	0.0008	0.0007
min	2.0000	2.0000	0.0058	0.0050
25%	7.0000	13.0000	0.0074	0.0058
50%	7.0000	14.0000	0.0077	0.0061
75%	7.0000	14.0000	0.0081	0.0063
max	7.0000	16.0000	0.0297	0.0297

7.3.3. Analysis of the behavior of the agents using RFn3

This RFn is a multi-objective function where, depending on the optimization profiles, an agent tries to minimize the associated cost of creating replicas or surpassing a threshold in latency. In the first optimization profile, the agents will try to balance the two objectives; in the second, the agents will optimize the creation of replicas, while in the last optimization profile, the agents will pay more attention to latency control. Therefore, three different behaviors are expected. Having multiple optimization profiles, a network solution designer can easily switch the agents' behavior so they optimize one objective, i.e., control the latency, or the other, i.e., limit the creation of replicas.

From Figures 9c, 9d, and 9e we can observe that the DQN agents are nicely stabilizing when using RFn3.1 and RFn3.3, with lower error margins. Conversely, the behavior of the PPO agents is more unstable, where convergence is still not reached in the mentioned cases. RFn3.2 is particularly difficult for PPO agents since they cannot keep a simulation running for the time that is intended (cf. Table 5).

This conclusion is also corroborated by the learning curve (see Figure 9d), where the normalized reward is even lower at the end of the 10 epochs than the untrained agent at epoch 0. In some cases of the RFn3.1 (cf. Table 5), the PPO is also not able to keep the simulation running, which may also explain the large error margins of Figure 9c. The same explanation is valid for the DQN case in the RFn3.2. The RFn3.3 seems to be the only RFn where both algorithms obtain a similar performance, despite the outlier of the DQN; notice, however, how the learning curve of Figure 9e does not capture this outlier.

Regarding the agents' behavior, as in the other RFns, we compare the best- and the worst-performing agents in each optimization profile. Since, according to Table 5, all DQN agents score the same for RFn3, the networking score helps in defining, in fact, which agent is performing the best. Table 11 shows *Run 2* of the DQN and the PPO for RFn3.1; Table 12 shows *Run 3* and *5* of the DQN for RFn3.2; and Table 13 shows *Run 2* of the PPO and *Run 3* of the DQN for RFn3.3.

From previous results, it is obvious that a scaling agent would need between 4.5 and 5 replicas to keep the latency under control. However, more than 5 replicas also accomplish the task, but with 4 replicas, the agent risks falling into the episode termination cases. Given how this RFn is proposed, RFn3.1 and RFn3.3 do not pose a limit in creating replicas. In contrast, RFn3.2 proposes a clear bound in the minimum number of replicas that keep a simulation running, disregarding the latency control.

We see this behavior clearly when looking at the agents of RFn3.2, where both DQN agents create four replicas on average, the minimum to keep the simulation running. Unfortunately, the PPO agents followed a greedier approach to maximizing the reward by minimizing the number of replicas beyond this point, falling into the episode termination cases. However, we can see that both agents do not control the latency as it is expected by the RFn design.

RFn3.1 shows a good balance between replica creation and latency control for both agents. Interestingly, the PPO agent manages the latency properly with fewer replicas than the DQN agent, except for a couple of times where the latency increased to a higher point than the DQN agent, and thus, it is hardly penalized. Notice that both agents are equally scored in learning (cf. Table 5), but it is in the networking score that both agents show their differences. In this RFn, once the latency is controlled, the PPO agents try to

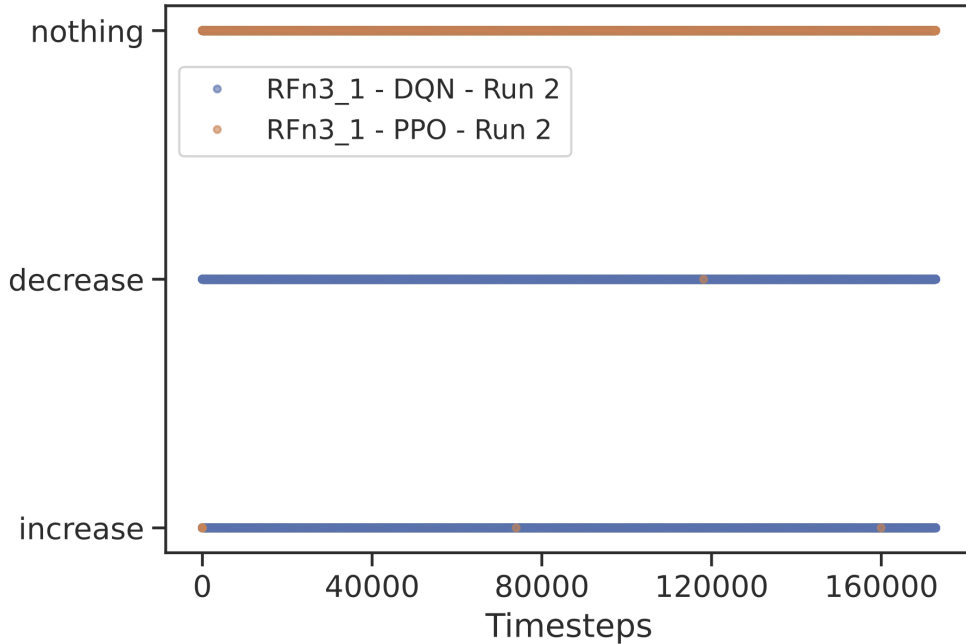


Figure 11: Action per step for the DQN (blue) and PPO (orange) agents using RFn3.1.

maintain the number of replicas untouched, as shown in Figure 11, yielding a zero reward most of the time. On the contrary, DQN agents keep searching for the right amount of replicas, which leads them to constantly change their actions, which is corroborated by the higher standard deviation in the replicas of their agents in Table 11.

In RFn3.3, the DQN agent in Table 13 exaggerates in the creation of replicas, but it seems that the agent has difficulties in choosing the number of replicas with which to exert latency control. On the other hand, the PPO agent is more moderate with the replicas, where during training, they tune the number of replicas that allow them to fulfill their objectives while keeping the simulation running, and then during testing, they keep the same number of replicas during the whole simulation time. Notice that although the PPO agent performs better regarding the number of replicas, the stability in their creation, and the latency control, they are scored similarly in learning and, in some cases, even less than their DQN counterparts.

7.3.4. Selecting the best-performing agent.

In the final selection phase, we identify the top-performing agents as follows: (i) DQN *Run 4* for RFn1, (ii) DQN *Run 3* for RFn2, (iii) DQN *Run 2* for RFn3.1, (iv) DQN *Run 5* for RFn3.2, and (v) PPO *Run 2* for RFn3.3. As suggested by our methodology, the next step is to we check if all the agents meet the criteria for deployment.

Firstly, the learning score criterion ensures that the chosen agents rank among the highest within their respective RFns. From Tables 5 and 6, only DQN *Run 4* with RFn1 and PPO *Run 2* with RFn3.3 achieve high scores in both learning and networking. Furthermore, analysis of the learning curves depicted in Figure 9 consistently demonstrates the superior performance of DQN agents trained with RFn1 compared to PPO agents, validating the selection of DQN *Run 4* for deployment.

8. Discussion

Future Zero-touch network and Service Management (ZSM) approaches will require an intelligence orchestrator [7] that autonomously (i) determines when a ML algorithm is ready for deployment, (ii) between

two or more algorithms, compares which algorithm performs better for a given task, and specifically for RL algorithms, (iii) assess the performance of two or more RFns. For doing that, a common approach is to compare and benchmark DRL algorithms based on the reward they receive in a well-defined and standard environment. However, in the previous section, we presented strong evidence that the reward might be insufficient to determine if two agents perform the same or differently or to select a better-performing algorithm. If this is not clear, the work of an orchestrator is much more difficult.

Regarding the first aspect, we realized that defining agent convergence to a stable reward value for a RL networking algorithm, especially for scaling, is not trivial. When referring to SL approaches, the training should stop before overfitting occurs. While some strategies to avoid overfitting, such as early stopping and regularization, are widely accepted in the SL community, such approaches are less clear in the RL community. We showed that depending on the RFn, the convergence to a stable value of the reward is not mandatory for an agent to achieve the two most common objectives in scaling, i.e., fulfilling an SLA with the lowest possible number of replicas.

Regarding the second aspect, we proposed a methodology encompassing the design of the DRL algorithms and the strategic definition of RFns. This methodology plays a crucial role in shaping the learning dynamics and performance of the scaling agents. The systematic assessment and empirical analysis demonstrate the potential of this approach in real-world applications. By identifying effective RFns and understanding the behavior of different algorithms, the methodology paves the way for developing more efficient and adaptable scaling agents. The comparison and analysis of different RFns and algorithms, as showcased in the experiments, are essential for refining the approach and achieving optimal performance.

Moreover, we defined a score based on the reward for faster identification of efficient agents. The scores generally corresponded to the stabilizing value of the normalized reward observed in the learning curves, created during training. This similarity in scoring across different RFns and algorithms suggests that the algorithms may be capable of finding similar policies regardless of their initial weight configurations. This insight is valuable in understanding the adaptability and robustness of DRL algorithms in different settings.

Furthermore, the score is good in ruling out agents that poorly behave, such as the PPO agents using RFn3.2. Moreover, the score is useful in comparing agents using the same RFn and algorithm, so it can rule out bad seeds such as the cases of the DQN agents using RFn3.2 and RFn3.3 and the PPO agents using RFn3.1. In addition, if there is a statistical difference in the performance of the algorithms, the score is good in determining which agent performs better, i.e., DQN outperforms PPO when using RFn1.

Nevertheless, in some particular cases, the learning score may be insufficient, since it may not be able to identify which of the agents are suitable for deployment, e.g., the PPO agents using RFn3.3 are similarly scored regarding learning, or it may not include the cases where the scaling is using other techniques than RL. For such cases, our methodology also includes the performance of the scaling task itself, in terms of the average number of created replicas and SLA compliance. However, as shown in [22], auto-scaling techniques lack a formal evaluation methodology, including a scoring metric for comparison and a widely accepted evaluation scenario. With the proposed methodology, we intend to close this gap, especially focusing on model selection for a completely autonomous network operation.

Finally, we showed that the RFn definition is a vital part of the lifecycle of DRL-based scaling algorithms. The default objective in a RL setup is to maximize the expected reward. As such, the expected reward is expressed as a sum where the order of the factors does not matter in the final result. However, the timely creation of the replicas is of the highest importance in scaling since if a replica is not created now, the latency might keep increasing. Thus, deciding when to create or delete a replica might heavily influence the agent's behavior in the long term, but this might not be reflected in the long-term reward. This also explains why an agent with better performance in the number of replicas and the latency control might receive a lower score than other agents with worse performance. Consequently, using different RFns with non-cumulative objectives [65] might produce better results than the ones we show in the previous section.

9. Conclusion and future research directions

ML algorithms stand at the forefront of transforming multiple facets of 6G, spanning network optimization, resource management, security, and user experience enhancement. As these algorithms become

inherent to all network segments, tackling diverse challenges, the demand for more efficient operation of NIFs intensifies. This integration signals a shift towards intelligent, self-organizing 6G networks capable of delivering unmatched performance, reliability, and scalability to meet the evolving needs of future applications and services. Consequently, establishing robust mechanisms for AI/ML performance evaluation, incorporating relevant parameters and KPIs, becomes imperative.

This paper proposes a methodology to design, train, validate, and select DRL algorithms with different RFns as autonomous agents and their use in networking. Moreover, the paper analyses the impact of the RFn definition on the behavior of DRL algorithms. As a study case, we chose to scale computing resources in service-based network architectures using such algorithms. For that purpose, we model the scaling problem as an MDP, being the main goal of the algorithms, to autonomously determine the number of replicas under a given constraint and constantly changing environment.

Moreover, we designed three RFns suitable to the scaling to guide the learning of each agent. Following common practices in the RL community, we experimentally evaluated the behavior of the DRL agents. We determined, when possible, the best-performing agent in terms of the replica creation and latency control. It was observed that only with RFn1 there is a consistent statistical difference across the epochs, with the DQN algorithm outperforming the PPO. This indicates that the choice of RFn significantly impacts the learning dynamics and effectiveness of DRL algorithms. However, for the other RFns, no definitive conclusions could be drawn, suggesting a need for more data to assess algorithm performance under these conditions reliably.

Additionally, we also showed how challenging it is to compare scaling algorithms in a fair way. Thus, we developed a methodology that includes the learning and the performance in the scaling task in terms of the number of created replicas and the SLA compliance. This methodology helps in performing autonomous model selection, a crucial step towards completely autonomous network operation, where ideally, the NI orchestrator should select the best-performing algorithm for this task. In that sense, our methodology extends current MLOps frameworks by considering multiple models designed with different RFns performing the same task.

Based on the literature analysis, we observe that the applicability of RL techniques in networking leave ample room for further innovation. Thus, as a contribution to closing that gap, we provided an abstraction layer to integrate two platforms, *OpenAI Gym*, the most used library to train and evaluate RL algorithms, and *DynamicSim*, a discrete-event simulator that enables the creation of edge-cloud network scenarios. With this abstraction layer, we created the playground on which scaling algorithms based on RL can be freely trained, tested, and compared.

Beyond improving the maturity of the methodology to compare and select scaling algorithms, even those that are not RL-based, there are still several open challenges. To widen the adoption of our benchmark environment, we need to extend *DynamicSim* to support more complex cases such as service function chaining where the NS is composed by multiple replicas, or the ability to migrate such NSs to comply with other types of KPIs such as energy consumption. An interesting extension is shown in [66], where multi-user workloads are considered in a neutral host service provider setup. Although limited, a real-life implementation is also one of the challenges. The abstraction layer of [31] and the evaluation methodology proposed in [67] could be used to implement RL algorithms for scaling. However, to avoid extra costs, the algorithm could first be trained in our benchmark to improve the quality of the algorithm's decisions.

Acknowledgment

Part of this research has been co-funded by the European Union's Horizon 2020 research and innovation program under Grant Agreement No. 101017109 (DAEMON), and No. 101136314 (6G-TWIN). However, views and opinions expressed are those of the author(s) only and do not necessarily reflect those of the European Union or Smart Networks and Services Joint Undertaking. Neither the European Union nor the granting authority can be held responsible for them.

This work has also received funding from the imec.icon project 5GECO. 5GECO is co-financed by imec and receives financial support from Flanders Innovation & Entrepreneurship (project nr. HBC.2021.0673) and/or Innoviris.

References

- [1] M. Giordani, M. Polese, M. Mezzavilla, S. Rangan, M. Zorzi, Toward 6g networks: Use cases and technologies, *IEEE Communications Magazine* 58 (3) (2020) 55–61.
- [2] T. Taleb, C. Benzaid, R. A. Addad, K. Samdanis, Ai/ml for beyond 5g systems: Concepts, technology enablers & solutions, *Computer Networks* 237 (2023) 110044.
- [3] E. Coronado, R. Behraves, T. Subramanya, A. Fernández-Fernández, M. S. Siddiqui, X. Costa-Pérez, R. Riggio, Zero touch management: A survey of network automation solutions for 5g and 6g networks, *IEEE Communications Surveys & Tutorials* 24 (4) (2022) 2535–2578.
- [4] M. Camelo, L. Cominardi, M. Gramaglia, M. Fiore, A. Garcia-Saavedra, L. Fuentes, D. De Vleeschauwer, P. Soto-Arenas, N. Slamnik-Krijestorac, J. Ballesteros, et al., Requirements and Specifications for the Orchestration of Network Intelligence in 6G, in: *2022 IEEE Annual Consumer Communications & Networking Conference (CCNC)*, IEEE, 2022, pp. 1–9.
- [5] ETSI, Zero-touch network and Service Management (ZSM); Reference Architecture, Group specification, ETSI (2019-08). URL <https://www.etsi.org/committee/zsm>
- [6] M. Camelo, M. Gramaglia, P. Soto, L. Fuentes, J. Ballesteros, A. Bazco-Nogueras, G. Garcia-Aviles, S. Latré, A. Garcia-Saavedra, M. Fiore, Daemon: A network intelligence plane for 6g networks, in: *2022 IEEE Globecom Workshops (GC Wkshps)*, IEEE, 2022, pp. 1341–1346.
- [7] L. E. Chatzieftheriou, M. Gramaglia, M. Camelo, A. Garcia-Saavedra, E. Kosmatos, M. Gucciardo, P. Soto, G. Iosifidis, L. Fuentes, G. Garcia-Aviles, et al., Orchestration procedures for the network intelligence stratum in 6g networks, in: *2023 Joint European Conference on Networks and Communications & 6G Summit (EuCNC/6G Summit)*, IEEE, 2023, pp. 347–352.
- [8] T. Zhang, M. Hemmatpour, S. Mishra, L. Linguaglossa, D. Zhang, C. S. Chen, M. Mellia, A. Aghasaryan, Operationalizing ai in future networks: A bird’s eye view from the system perspective, *arXiv preprint arXiv:2303.04073* (2023).
- [9] Z. Chen, K. He, J. Li, Y. Geng, Seq2Img: A sequence-to-image based approach towards IP traffic classification using convolutional neural networks, in: *2017 IEEE International Conference on Big Data (Big Data)*, 2017, pp. 1271–1276. doi:10.1109/BigData.2017.8258054.
- [10] M. Camelo, P. Soto, S. Latré, A General Approach for Traffic Classification in Wireless Networks Using Deep Learning, *IEEE Transactions on Network and Service Management* 19 (4) (2022) 5044–5063. doi:10.1109/TNSM.2021.3130382.
- [11] P. Li, J. Thomas, X. Wang, A. Khalil, A. Ahmad, R. Inacio, S. Kapoor, A. Parekh, A. Doufexi, A. Shojaefard, et al., RLOps: Development life-cycle of reinforcement learning aided open RAN, *IEEE Access* 10 (2022) 113808–113826.
- [12] U. Altaf, G. Jayaputera, J. Li, D. Marques, D. Meggyesy, S. Sarwar, S. Sharma, W. Voorsluys, R. Sinnott, A. Novak, et al., Auto-scaling a defence application across the cloud using docker and kubernetes, in: *2018 IEEE/ACM International Conference on Utility and Cloud Computing Companion (UCC Companion)*, IEEE, 2018, pp. 327–334.
- [13] M. Gotin, F. Löscher, R. Heinrich, R. Reussner, Investigating performance metrics for scaling microservices in cloudiot-environments, in: *Proceedings of the 2018 ACM/SPEC International Conference on Performance Engineering*, 2018, pp. 157–167.
- [14] D. Kreuzberger, N. Kühl, S. Hirschl, Machine learning operations (MLOps): Overview, definition, and architecture, *IEEE Access* (2023).
- [15] P. Kurrek, F. Zoghiami, M. Jocas, M. Stoelen, V. Salehi, Q-model: An artificial intelligence based methodology for the development of autonomous robots, *Journal of Computing and Information Science in Engineering* 20 (6) (2020) 061006.
- [16] O-RAN WG2, O-RAN AI/ML workflow description and requirements - v1.02, Technical report, O-RAN (2020).
- [17] A. Raffin, A. Hill, A. Gleave, A. Kanervisto, M. Ernestus, N. Dormann, Stable-baselines3: Reliable reinforcement learning implementations, *The Journal of Machine Learning Research* 22 (1) (2021) 12348–12355.
- [18] G. Brockman, V. Cheung, L. Pettersson, J. Schneider, J. Schulman, J. Tang, W. Zaremba, Openai gym, *arXiv preprint arXiv:1606.01540* (2016).
- [19] P. Gawlowicz, A. Zubow, Ns-3 meets openai gym: The playground for machine learning in networking research, in: *Proceedings of the 22nd International ACM Conference on Modeling, Analysis and Simulation of Wireless and Mobile Systems*, 2019, pp. 113–120.
- [20] T. Subramanya, R. Riggio, Centralized and federated learning for predictive vnf autoscaling in multi-domain 5g networks and beyond, *IEEE Transactions on Network and Service Management* 18 (1) (2021) 63–78.
- [21] J. Martín-Pérez, K. Kondepu, D. De Vleeschauwer, V. Reddy, C. Guimarães, A. Sgambelluri, L. Valcarengi, C. Pagianni, C. J. Bernardos, Dimensioning of v2x services in 5g networks through forecast-based scaling, *arXiv preprint arXiv:2105.12527* (2021).
- [22] T. Lorido-Botran, J. Miguel-Alonso, J. A. Lozano, A review of auto-scaling techniques for elastic applications in cloud environments, *Journal of grid computing* 12 (4) (2014) 559–592.
- [23] T. Chen, R. Bahsoon, X. Yao, A survey and taxonomy of self-aware and self-adaptive cloud autoscaling systems, *arXiv preprint arXiv:1609.03590* (2016).
- [24] T. L. Duc, R. G. Leiva, P. Casari, P.-O. Östberg, Machine learning methods for reliable resource provisioning in edge-cloud computing: A survey, *ACM Computing Surveys (CSUR)* 52 (5) (2019) 1–39.
- [25] Y. Garí, D. A. Monge, E. Pacini, C. Mateos, C. G. Garino, Reinforcement learning-based application autoscaling in the cloud: A survey, *Engineering Applications of Artificial Intelligence* 102 (2021) 104288.
- [26] F. Rossi, M. Nardelli, V. Cardellini, Horizontal and vertical scaling of container-based applications using reinforcement learning, in: *2019 IEEE 12th International Conference on Cloud Computing (CLOUD)*, IEEE, 2019, pp. 329–338.
- [27] L. He, L. Li, Y. Liu, Towards chain-aware scaling detection in nfv with reinforcement learning, in: *2021 IEEE/ACM 29th International Symposium on Quality of Service (IWQOS)*, IEEE, 2021, pp. 1–10.

- [28] A. A. Khaleq, I. Ra, Intelligent autoscaling of microservices in the cloud for real-time applications, *IEEE Access* 9 (2021) 35464–35476.
- [29] P. Soto, D. De Vleeschauwer, M. Camelo, Y. De Bock, K. De Schepper, C.-Y. Chang, P. Hellinckx, J. F. Botero, S. Latré, Towards autonomous VNF auto-scaling using deep reinforcement learning, in: 2021 Eighth International Conference on Software Defined Systems (SDS), IEEE, 2021, pp. 01–08.
- [30] P. Soto, M. Camelo, D. De Vleeschauwer, Y. De Bock, C.-Y. Chang, J. F. Botero, S. Latré, Network Intelligence for NFV Scaling in Closed-Loop Architectures, *IEEE Communications Magazine* 61 (6) (2023) 66–72.
- [31] J. Santos, T. Wauters, B. Volckaert, F. De Turck, gym-hpa: Efficient auto-scaling via reinforcement learning for complex microservice-based applications in kubernetes, in: NOMS 2023-2023 IEEE/IFIP Network Operations and Management Symposium, IEEE, 2023, pp. 1–9.
- [32] J. Deng, W. Dong, R. Socher, L.-J. Li, K. Li, L. Fei-Fei, Imagenet: A large-scale hierarchical image database, in: 2009 IEEE conference on computer vision and pattern recognition, Ieee, 2009, pp. 248–255.
- [33] Y. Tay, M. Dehghani, S. Abnar, Y. Shen, D. Bahri, P. Pham, J. Rao, L. Yang, S. Ruder, D. Metzler, Long range arena: A benchmark for efficient transformers, arXiv preprint arXiv:2011.04006 (2020).
- [34] P. Warden, Speech commands: A dataset for limited-vocabulary speech recognition, arXiv preprint arXiv:1804.03209 (2018).
- [35] P. Henderson, R. Islam, P. Bachman, J. Pineau, D. Precup, D. Meger, Deep reinforcement learning that matters, in: Proceedings of the AAAI conference on artificial intelligence, Vol. 32(1), 2018, pp. 3207–3214.
- [36] R. Islam, P. Henderson, M. Gomrokchi, D. Precup, Reproducibility of benchmarked deep reinforcement learning tasks for continuous control, arXiv preprint arXiv:1708.04133 (2017).
- [37] G. F. Riley, T. R. Henderson, The ns-3 network simulator, in: Modeling and tools for network simulation, Springer, 2010, pp. 15–34.
- [38] Google, Protocol Buffers, accessed: 2024-03-28 (2024).
URL <https://protobuf.dev/>
- [39] H. Yin, P. Liu, K. Liu, L. Cao, L. Zhang, Y. Gao, X. Hei, ns3-ai: Fostering artificial intelligence algorithms for networking research, in: Proceedings of the 2020 Workshop on ns-3, 2020, pp. 57–64.
- [40] L. Bonati, M. Polese, S. D’Oro, S. Basagni, T. Melodia, OpenRAN Gym: AI/ML development, data collection, and testing for O-RAN on PAWR platforms, *Computer Networks* 220 (2023) 109502.
- [41] L. Bonati, P. Johari, M. Polese, S. D’Oro, S. Mohanti, M. Tehrani-Moayyed, D. Villa, S. Shrivastava, C. Tassie, K. Yoder, et al., Colosseum: Large-scale wireless experimentation through hardware-in-the-loop network emulation, in: 2021 IEEE International Symposium on Dynamic Spectrum Access Networks (DySPAN), IEEE, 2021, pp. 105–113.
- [42] M. Miozzo, N. Bartzoudis, M. Requena, O. Font-Bach, P. Harbanau, D. López-Bueno, M. Payaró, J. Mangues, SDR and NFV extensions in the ns-3 LTE module for 5G rapid prototyping, in: 2018 IEEE Wireless Communications and Networking Conference (WCNC), IEEE, 2018, pp. 1–6.
- [43] W. Garey, T. Ropitault, R. Rouil, E. Black, W. Gao, O-RAN with Machine Learning in ns-3, in: Proceedings of the 2023 Workshop on ns-3, 2023, pp. 60–68.
- [44] K. Mehmood, K. Kravlevska, D. Palma, Intent-driven autonomous network and service management in future cellular networks: A structured literature review, *Computer Networks* 220 (2023) 109477.
- [45] F. Wilhelmi, M. Carrascosa, C. Cano, A. Jonsson, V. Ram, B. Bellalta, Usage of Network Simulators in Machine-Learning-Assisted 5G/6G Networks, *IEEE Wireless Communications* 28 (1) (2021) 160–166.
- [46] P. Almasan, M. Ferriol-Galmes, J. Paillisse, J. Suarez-Varela, D. Perino, D. Lopez, A. A. P. Perales, P. Harvey, L. Ciavaglia, L. Wong, V. Ram, S. Xiao, X. Shi, X. Cheng, A. Cabellos-Aparicio, P. Barlet-Ros, Network digital twin: Context, enabling technologies and opportunities, *IEEE Communications Magazine* (2022) 1–13doi:10.1109/MCOM.001.2200012.
- [47] L. Engstrom, A. Ilyas, S. Santurkar, D. Tsipras, F. Janoos, L. Rudolph, A. Madry, Implementation matters in Deep RL: A case study on PPO and TRPO, in: International Conference on Learning Representations, 2020, pp. 1–14.
URL <https://openreview.net/forum?id=r1etN1rtPB>
- [48] N. C. Luong, D. T. Hoang, S. Gong, D. Niyato, P. Wang, Y.-C. Liang, D. I. Kim, Applications of deep reinforcement learning in communications and networking: A survey, *IEEE Communications Surveys & Tutorials* 21 (4) (2019) 3133–3174.
- [49] M. S. Bonfim, K. L. Dias, S. F. Fernandes, Integrated NFV/SDN architectures: A systematic literature review, *ACM Computing Surveys (CSUR)* 51 (6) (2019) 1–39.
- [50] O. Adamuz-Hinojosa, J. Ordóñez-Lucena, P. Ameigeiras, J. J. Ramos-Munoz, D. Lopez, J. Figueira, Automated network service scaling in nfv: Concepts, mechanisms and scaling workflow, *IEEE Communications Magazine* 56 (7) (2018) 162–169.
- [51] O. Gheibi, D. Weyns, F. Quin, Applying machine learning in self-adaptive systems: A systematic literature review, *ACM Transactions on Autonomous and Adaptive Systems (TAAS)* 15 (3) (2021) 1–37.
- [52] R. S. Sutton, A. G. Barto, Reinforcement learning: An introduction, MIT press, 2018.
- [53] C. J. Watkins, P. Dayan, Q-learning, *Machine learning* 8 (1992) 279–292.
- [54] K. Arulkumaran, M. P. Deisenroth, M. Brundage, A. A. Bharath, Deep reinforcement learning: A brief survey, *IEEE Signal Processing Magazine* 34 (6) (2017) 26–38.
- [55] V. Mnih, K. Kavukcuoglu, D. Silver, A. A. Rusu, J. Veness, M. G. Bellemare, A. Graves, M. Riedmiller, A. K. Fidjeland, G. Ostrovski, et al., Human-level control through deep reinforcement learning, *nature* 518 (7540) (2015) 529–533.
- [56] J. Schulman, F. Wolski, P. Dhariwal, A. Radford, O. Klimov, Proximal policy optimization algorithms, arXiv preprint arXiv:1707.06347 (2017).
- [57] V. Mnih, K. Kavukcuoglu, D. Silver, A. Graves, I. Antonoglou, D. Wierstra, M. Riedmiller, Playing atari with deep

- reinforcement learning, arXiv preprint arXiv:1312.5602 (2013).
- [58] T. Song, D. Kaleshi, R. Zhou, O. Boudeville, J.-X. Ma, A. Pelletier, I. Haddadi, Performance evaluation of integrated smart energy solutions through large-scale simulations, in: 2011 IEEE International Conference on Smart Grid Communications (SmartGridComm), IEEE, 2011, pp. 37–42.
 - [59] J. Achiam, Spinning up in Deep Reinforcement Learning, <https://spinningup.openai.com/>, accessed: 2024-01-03 (2018).
 - [60] C. Colas, O. Sigaud, P.-Y. Oudeyer, How many random seeds? statistical power analysis in deep reinforcement learning experiments, arXiv preprint arXiv:1806.08295 (2018).
 - [61] C. Colas, O. Sigaud, P.-Y. Oudeyer, A hitchhiker’s guide to statistical comparisons of reinforcement learning algorithms, arXiv preprint arXiv:1904.06979 (2019).
 - [62] P. Rochet, I. Serra, The mean/max statistic in extreme value analysis, arXiv preprint arXiv:1606.08974 (2016).
 - [63] Y. Yu, Towards Sample Efficient Reinforcement Learning., in: Proceedings of the 27th International Joint Conference on Artificial Intelligence, 2018, pp. 5739–5743.
 - [64] J. Eschmann, Reward function design in Reinforcement Learning, Reinforcement Learning Algorithms: Analysis and Applications (2021) 25–33.
 - [65] W. Cui, W. Yu, Reinforcement Learning with Non-Cumulative Objective, IEEE Transactions on Machine Learning in Communications and Networking (2023).
 - [66] J. Jimenez, P. Soto, D. De Vleeschauwer, C.-Y. Chang, Y. De Bock, S. Latre, M. Camelo, Resource Allocation of Multi-User Workloads in Cloud and Edge Data-Centers Using Reinforcement Learning, in: 19th International Conference on Network and Service Management (CNSM), IEEE, 2023, pp. 1–5.
 - [67] V. Zalokostas-Diplas, N. Makris, V. Passas, T. Korakis, Experimental evaluation of ml models for dynamic vnf autoscaling, in: 2022 IEEE Conference on Standards for Communications and Networking (CSCN), IEEE, 2022, pp. 157–162.